

PL-TR-97-2125

**DIFFICULT WEATHER: A REVIEW OF THUNDERSTORM, FOG AND
STRATUS, AND WINTER PRECIPITATION FORECASTING**

**Monique G. Venne
William H. Jasperson
David E. Venne**

**Augsburg College
Center for Atmospheric and Space Sciences
2211 Riverside Avenue
Minneapolis, MN 55454**

30 September 1997

**6 July 1995 – 30 September 1997
Final Report**

APPROVED FOR PUBLIC RELEASE; DISTRIBUTION UNLIMITED

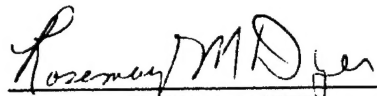
DTIC QUALITY INSPECTED 3

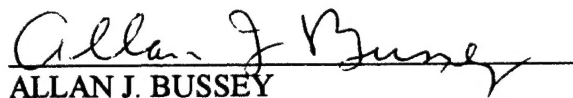


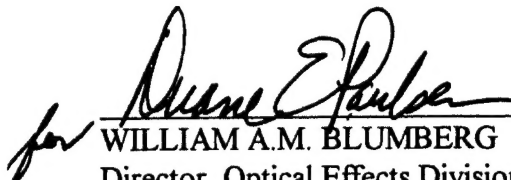
**PHILLIPS LABORATORY
Directorate of Geophysics
AIR FORCE MATERIEL COMMAND
HANSCOM AFB, MA 01731-3010**

19980202 037

This technical report has been reviewed and is approved for publication.


ROSEMARY M. DYER
Contract Manager


ALLAN J. BUSSEY
Acting Chief, Forecast Applications Branch


WILLIAM A.M. BLUMBERG
Director, Optical Effects Division

This report has been reviewed by the ESC Public Affairs Office (PA) and is releasable to the National Technical Information Service (NTIS).

Qualified requesters may obtain additional copies from the Defense Technical Information Center (DTIC). All others should apply to the NTIS.

If your address has changed, if you wish to be removed from the mailing list, or if the addressee is no longer employed by your organization, please notify PL/TSI, 29 Randolph Road, Hanscom AFB, MA 01731-3010. This will assist us in maintaining a current mailing list.

Do not return copies of this report unless contractual obligations or notices on a specific document require that it be returned.

TABLE OF CONTENTS

| | |
|--|----|
| 1. INTRODUCTION | 1 |
| 2. THUNDERSTORMS | 1 |
| 2.1 Introduction | 1 |
| 2.2 Description | 6 |
| 2.3 Moisture Parameters | 7 |
| 2.4 Stability and Kinetic Indices | 7 |
| 2.5 Sources of Lift | 14 |
| 2.6 Assessing Severe Weather Potential | 17 |
| 3. FOG AND STRATUS | 19 |
| 3.1 Introduction | 19 |
| 3.2 Radiation Fogs | 25 |
| 3.3 Advection Fogs | 26 |
| 3.4 Frontal Fogs | 29 |
| 3.5 Fog Forecasting Methods | 30 |
| 4. WINTER PRECIPITATION | 34 |
| 4.1 Introduction | 34 |
| 4.2 The Rain/Snow Line | 34 |
| 4.3 Freezing Rain and Ice Pellets | 36 |
| 4.4 Snow Accumulation | 38 |
| 5. SUMMARY | 39 |
| 6. BIBLIOGRAPHY | 40 |
| 6.1 Introductory References | 40 |
| 6.2 Thunderstorm References | 40 |
| 6.3 Fog References | 43 |
| 6.4 Winter Precipitation References | 46 |

LIST OF FIGURES

| | | |
|---|---|----|
| 1 | Average number of days with thunderstorms, January (Guttman 1971) | 2 |
| 2 | Average number of days with thunderstorms, April (Guttman 1971) | 3 |
| 3 | Average number of days with thunderstorms, July (Guttman 1971) | 4 |
| 4 | Average number of days with thunderstorms, October (Guttman 1971) | 5 |
| 5 | Percentage frequency of occurrence of fog, January (Guttman 1971) | 21 |
| 6 | Percentage frequency of occurrence of fog, April (Guttman 1971) | 22 |
| 7 | Percentage frequency of occurrence of fog, July (Guttman 1971) | 23 |
| 8 | Percentage frequency of occurrence of fog, October (Guttman 1971) | 24 |

LIST OF TABLES

| | | |
|----|---|----|
| 1 | Moisture parameters and values needed to initiate DMC | 7 |
| 2 | K-Index values and thunderstorm probabilities in United States | 8 |
| 3 | Showalter Index values and probable thunderstorm intensities for United States | 8 |
| 4 | Lifted Index values and probable thunderstorm intensities for United States ... | 9 |
| 5 | Vertical Totals threshold values for North America and western Europe | 9 |
| 6 | Vertical Totals values and extent of thunderstorm activity in mountainous regions when significant moisture is present | 10 |
| 7 | Total Total values and expected thunderstorm activity for United States | 10 |
| 8 | Helicity values and expected tornado intensities in United States | 13 |
| 9 | Jet heights, wind speeds, and expected thunderstorm severity for United States | 15 |
| 10 | Fog Stability Index values and the likelihood of radiation fog | 31 |
| 11 | Fog Threat values and the likelihood of radiation fog | 32 |
| 12 | Thickness layers and the corresponding critical thickness values to discriminate between rain and snow in the United States | 35 |
| 13 | Surface visibility during snowfall and average hourly snow accumulation | 38 |

In memory of
W. KEITH HENRY
1919-1997

1. INTRODUCTION

This report is the result of an investigation into the forecasting of three weather events that have been traditionally considered to be difficult to forecast, namely thunderstorms, fog, and winter precipitation. These events tend to be local phenomena of relatively short-term duration, and are disruptive when they occur over airfields. The motivation for this study was to examine forecast methods for these events that use only locally or regionally available data. Modern meteorologists use a vast array of data sources, ranging from global surface and upper air data, to radar and satellite images, to sophisticated numerical models, in order to generate a weather forecast. Knowledge of how to use limited data to forecast difficult weather, called *single-station forecasting* by Oliver and Oliver (1945), is critical during any military scenario if communications are disrupted or links to other sources of meteorological data and forecasts are broken.

This report contains no original research, but is a compilation of objective methods and "rules of thumb" that have been developed for forecasting thunderstorms, fog, and winter precipitation. The formal and informal literature has been surveyed to find as many suitable techniques as possible. The remainder of this report describes these difficult-to-forecast weather events and various ways employed to forecast them. An extensive bibliography is provided at the end of the report.

2. THUNDERSTORMS

2.1 Introduction

Thunderstorms are considered to be the most serious weather hazard to aviation (Braham 1996). At flight level they can cause severe turbulence, hail, icing, and power failures due to lightning strikes. During takeoffs and landings, additional thunderstorm hazards include microbursts, wind shear, heavy rain, and flash flooding. Severe thunderstorms typically have wind gusts greater than 26 m sec^{-1} (50 kts) and the potential to spawn tornadoes.

For those who fly regularly, thunderstorms cannot always be avoided. Figures 1 through 4 show global charts with the average number of days with thunderstorms for January, April, July, and October, respectively (Guttman 1971). As expected, there are large numbers of thunderstorms in the Tropics (30°N - 30°S) throughout the year. The mid-latitude regions of the Northern Hemisphere continents (30°N - 60°N) are also affected by thunderstorms throughout most of the year. In July (Fig. 3), almost all the land areas south of 60°N have an average of at least five thunderstorm days. The Southern Hemisphere, which has most of its land area in the Tropics, shows thunderstorm "hot spots" moving seasonally with the Intertropical Convergence Zone.

The vast majority of thunderstorm research has been conducted in the United States, but the findings from this research have been applicable in other parts of the world. Dessens and Snow (1989) pointed out that many of the tornadoes in France developed with the same kind of conditions as documented for tornadoes in the central United States. Jacovides and

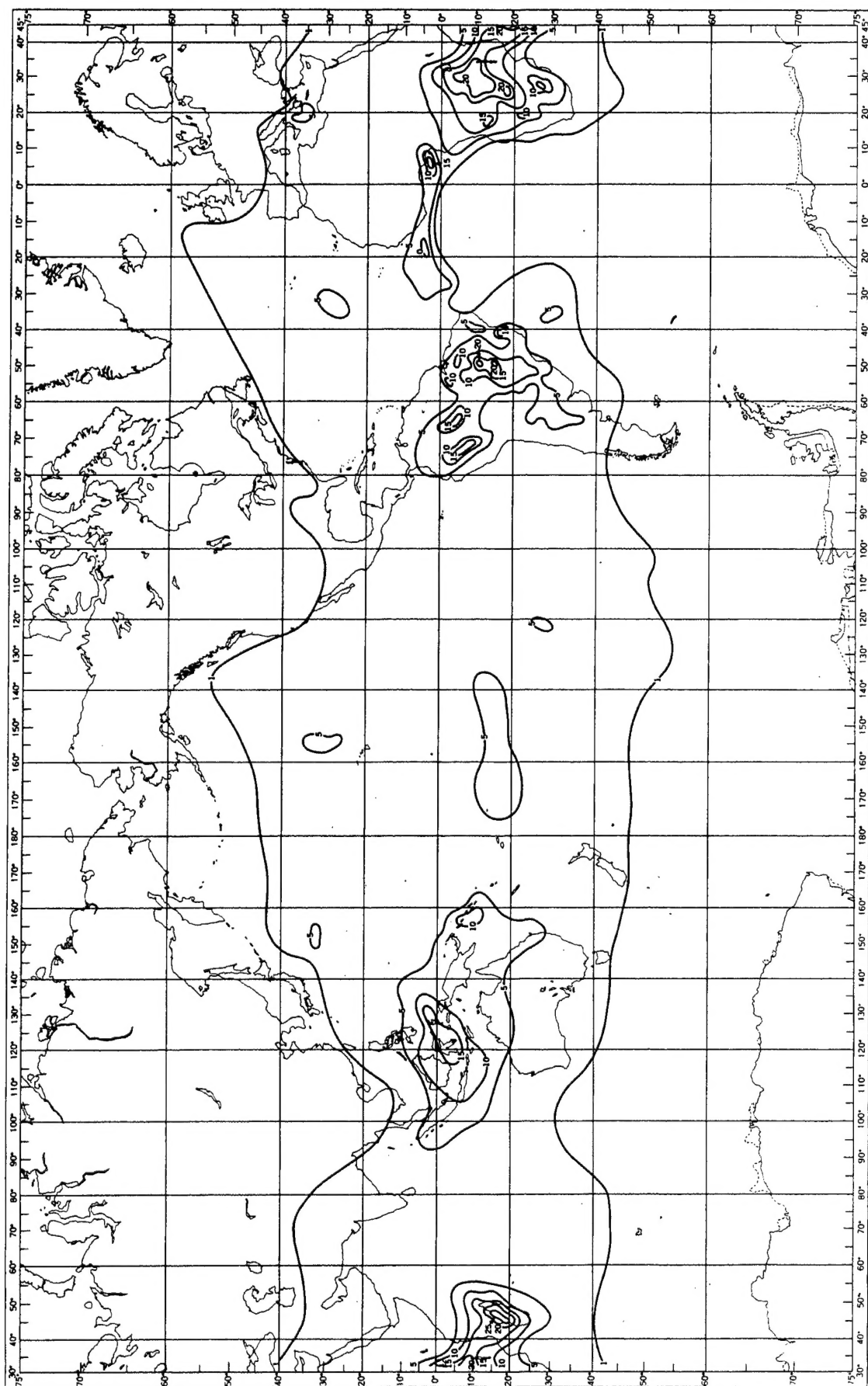


Figure 1. Average number of days with thunderstorms, January (From Guttman 1971)

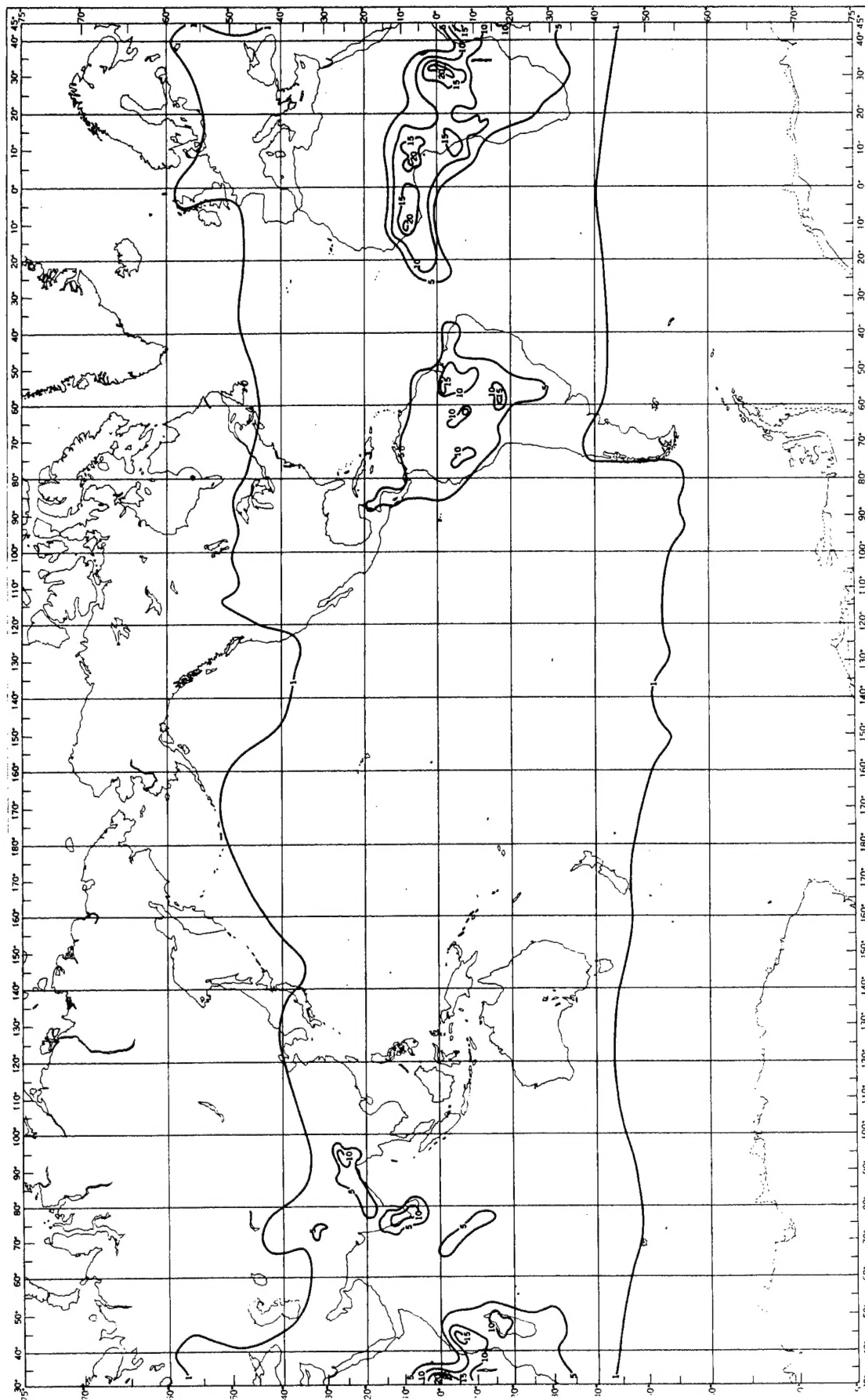


Figure 2. Average number of days with thunderstorms, April (From Guttman 1971)

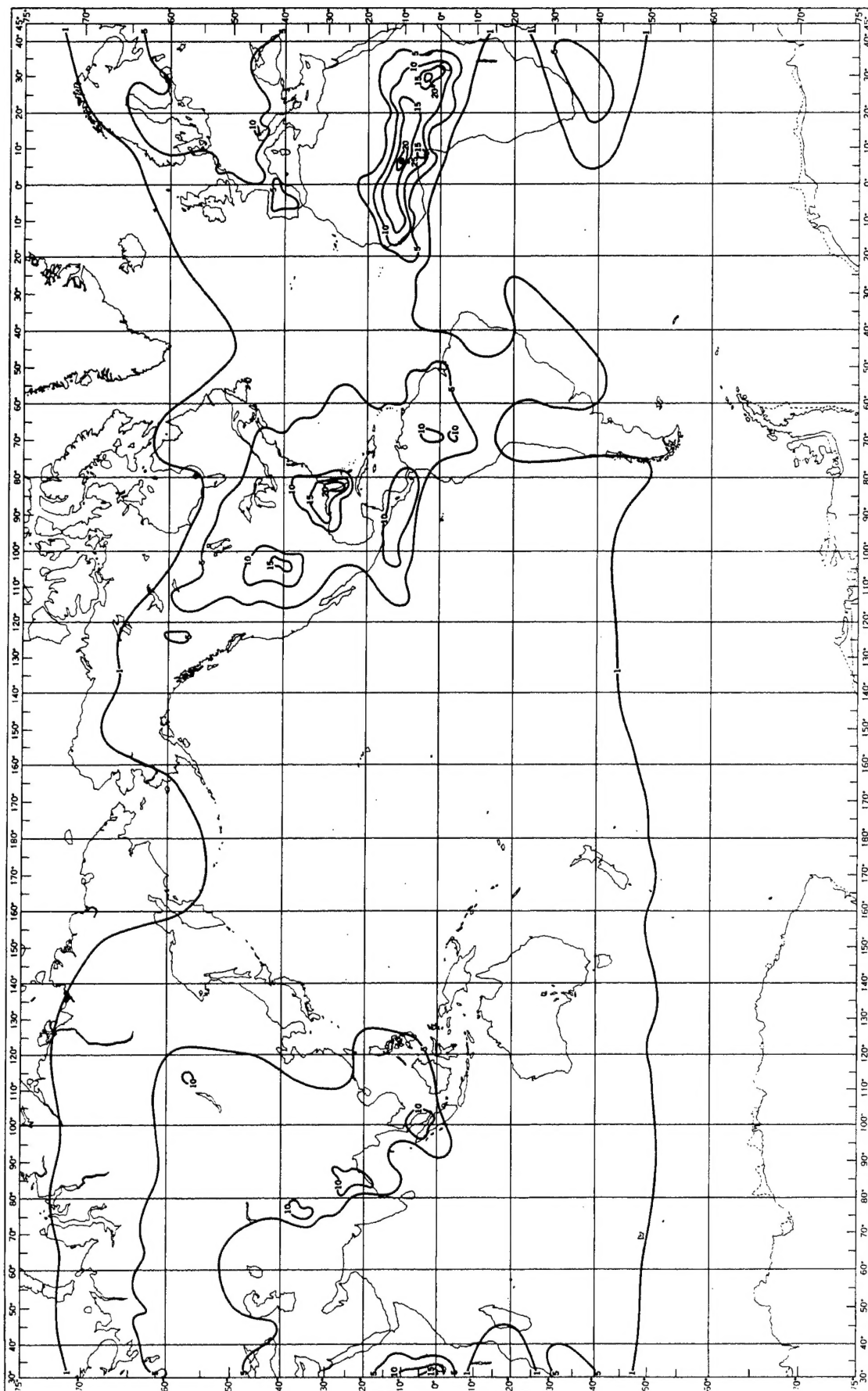


Figure 3. Average number of days with thunderstorms, July (From Guttman 1971)

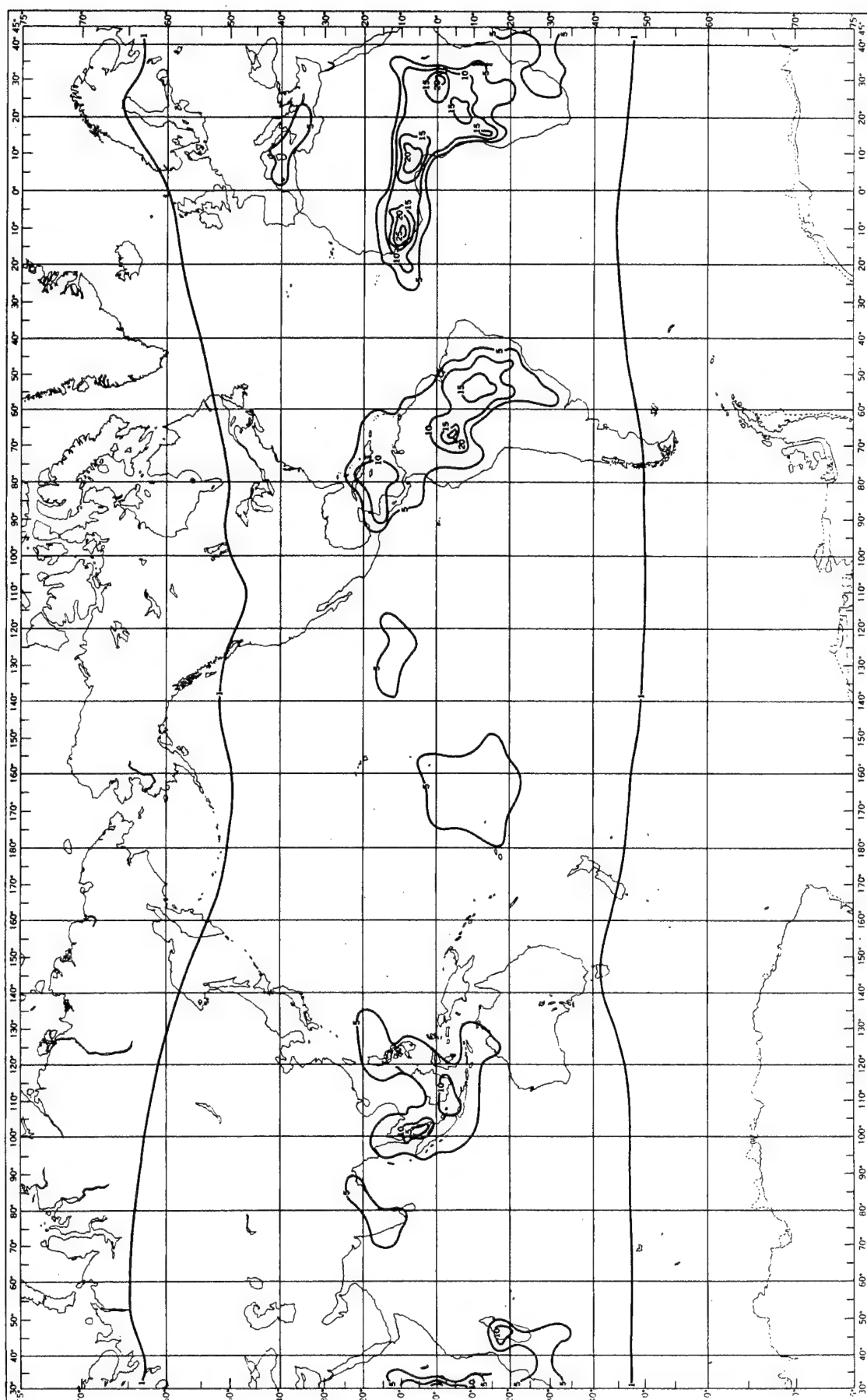


Figure 4. Average number of days with thunderstorms, October (From Guttman 1971)

Yonetani (1990) found that combining a thermodynamic index with a kinematic parameter improved the skill of forecasting non-frontal thunderstorms in Cyprus. Huntrieser et al. (1997) discovered that the Showalter Index at 00Z and SWEAT Index at 12Z had the highest skill scores of the traditional stability indices for predicting thunderstorms in Switzerland. Tudurí and Ramis (1997) used CAPE and helicity to classify thunderstorm environments in the western Mediterranean.

2.2 Description

Thunderstorms are the product of deep moist convection (DMC). The three necessary ingredients for DMC are (Johns and Doswell 1992):

- a moist layer of sufficient depth (at least 100 mb) in the low or mid-troposphere
- a steep enough lapse rate (greater than moist adiabatic in the mid-troposphere) to allow for a substantial "positive area"
- sufficient lifting of a parcel from the moist layer to allow it to reach its level of free convection (LFC).

A severe thunderstorm is defined as having at least one of the following events (Johns and Doswell 1992):

- tornadoes
- damaging winds, or wind gusts ≥ 26 m/sec (50 kts)
- hail with diameter ≥ 1.9 cm (0.75 in)

Three factors differentiate the severe thunderstorm environment from the non-severe thunderstorm environment (McNulty 1995):

- extreme instability
- strong vertical wind shear
- mid-level dry air or intrusion of dry air at mid-levels.

For thunderstorm forecasting purposes, it should first be determined whether DMC can be expected. If DMC is probable, the possibility for mesocyclone formation and severe weather is then evaluated (Moller et al. 1994).

Thunderstorm forecasting begins with examination of the moisture and temperature profiles of an upper air sounding. Next, a parcel is lifted to calculate some of the stability indices. There have been many discussions as to how to determine the best parcel to lift. Some of the suggested parcels have been a parcel with surface parameters, a parcel with mean parameters of the near-surface layer (with the depth of the layer varying from 35 mb to 100 mb), and the most unstable parcel below 300 mb (Doswell and Rasmussen 1994). The National Weather Service lifts a parcel with mean potential temperature and mixing ratio of the lowest 100 mb for operational use (Hart and Korotky 1991). If thunderstorms are anticipated, a parcel with the properties of the current surface temperature and dewpoint should be lifted every hour and the stability indices recalculated (Hales and Doswell 1982). When doing so, the original sounding must be modified in the boundary layer to take diurnal heating/cooling and advection into account (McGinley 1986, Moore and Pino 1990). The vertical wind profile, or

hodograph, also needs to be examined to determine the character of possible thunderstorms given a favorable thermodynamic environment (Doswell 1991).

2.3 Moisture Parameters

Table 1 lists different moisture parameters and the critical values at different levels needed to initiate DMC (Miller 1972, Modahl 1979, Johns 1986).

Table 1. Moisture parameters and values needed to initiate DMC

| <i>Parameter</i> | <i>Sfc</i> | <i>850 mb</i> | <i>700 mb</i> | <i>500 mb</i> |
|--------------------------------------|---|--|---|----------------------------|
| Dewpoint temp | $\geq 13^{\circ}\text{C}$ (elev. < 3500 ft) | $\geq 8^{\circ}\text{C}$ | $\geq 0^{\circ}\text{C}$ (svr: < 0°C) | $\geq -17^{\circ}\text{C}$ |
| Dewpoint depression | | $< 15^{\circ}\text{C}$ (svr: < 5°C) | $\leq 6^{\circ}\text{C}$ (svr: > 6°C) | $\leq 6^{\circ}\text{C}$ |
| Mean relative humidity | 40%-80% (svr: 50%-70%) (0-3000 ft AGL) | | $\geq 50\%$ (svr: < 50%) | $\geq 50\%$ |
| Mean mixing ratio (0-3000 ft AGL) | $> 8 \text{ g/kg}$ (svr: > 12 g/kg) (elev. < 3500 ft) | $> 4 \text{ g/kg}$ (svr: > 9 g/kg) (elev. > 3500 ft) | | |
| Precipitable water | $> 0.50 \text{ in.}$ (svr: > 0.70 in.) | | | |

2.4 Stability and Kinetic Indices

NOTE: When station elevation is greater than 1000 gpm, use the following base levels for computing indices requiring data from 850 mb (US Dept. of Commerce 1969):

- 1000-1400 gpm 800 mb
- 1401-2000 gpm 750 mb

2.4.1 K Index

The K-Index (KI) is used in determining the probability of non-severe thunderstorms which occur without an obvious source of lift, and especially favors heavy rain-producing convection (Air Weather Service 1979, Hart and Korotky 1991). It is calculated by

$$\text{KI} = T_{850} - T_{500} + T_{d850} - T_{dd700}, \quad (1)$$

where

- T_{850} = 850 mb temperature ($^{\circ}\text{C}$)
- T_{500} = 500 mb temperature ($^{\circ}\text{C}$)
- T_{d850} = 850 mb dew point temperature ($^{\circ}\text{C}$)
- T_{dd700} = 700 mb dew point depression ($^{\circ}\text{C}$)

KI values and the corresponding thunderstorm probabilities for the United States are listed in Table 2. Note that a low KI value in the presence of other severe weather indicators suggests severe weather development because it indicates the presence of the 700 mb dry tongue.

Table 2. K-Index values and thunderstorm probabilities in United States

| <i>K Index West of Rockies</i> | <i>K Index East of Rockies</i> | <i>Airmass Tstorm Probability</i> |
|------------------------------------|------------------------------------|---------------------------------------|
| <15 | <20 | near 0% |
| 15 to 20 | 20 to 25 | <20% |
| 21 to 25 | 26 to 30 | 20-40% |
| 26 to 30 | 31 to 35 | 40-60% |
| 31 to 35 | 36 to 40 | 60-80% |
| 36 to 40 | 41 to 45 | 80-90% |
| >40 | >45 | near 100% |

2.4.2 Showalter Index

The Showalter Index (SI) assesses the potential instability of the 850-500 mb layer. It is computed by lifting a parcel adiabatically from 850 mb to 500 mb and taking the difference between the parcel temperature and the sounding temperature at 500 mb. It is most useful when a shallow cool airmass below 850 mb conceals greater convective potential aloft (Hart and Korotky 1991). Table 3 lists the critical values established for the United States (Air Weather Service 1979, Baker and Schlatter 1986).

Table 3. Showalter Index values and probable thunderstorm intensities for United States

| <i>Showalter Value</i> | <i>Thunderstorm indications</i> |
|------------------------|--|
| 3 to 1 | tstms possible – good trigger mechanism needed |
| 0 to -3 | unstable – tstms probable |
| -4 to -6 | very unstable – good hvy tstm potential |
| <-6 | extremely unstable – good svr tstm potential |

2.4.3 Lifted Index

The Lifted Index (LI) is used as a gauge of thunderstorm severity. It was developed as a modification of the SI because the 850 mb level does not always represent the boundary layer. It is calculated by lifting a parcel with mean boundary layer conditions adiabatically to 500 mb and taking the difference between the parcel temperature and the sounding temperature at 500 mb. In operational use, a parcel based on the mean temperature and mixing ratio of the lowest 100 mb is used to determine the LI at the sounding time. Between soundings, a surface-based parcel is lifted and the LI is calculated with a modified sounding (see Section 2.2). Table 4 lists LI values using a mean boundary layer parcel and the probable thunderstorm intensities for the United States. Note that the LI using surface parcels will typically have lower values; i.e., be more unstable (Air Weather Service 1979, Baker and Schlatter 1986).

Table 4. Lifted Index values and probable thunderstorm intensities for United States

| <i>Lifted Index Value</i> | <i>Thunderstorm indications</i> |
|---------------------------|--|
| > +2 | no convective activity |
| 0 to +2 | showers probable, isolated tstms possible |
| -2 to 0 | tstms possible – good trigger mechanism needed |
| -4 to -2 | tstms probable, svr tstms possible |
| -6 to -4 | svr tstms probable, tornadoes possible |
| <-6 | tornadoes probable |

In the western United States (roughly west of 105°W), surface-based LI values less than zero and surface dewpoint temperatures greater than 11°C (52°F) indicate the possibility of severe thunderstorms (Hales 1985).

2.4.4 Vertical Totals

The Vertical Totals (VT) measures the 850-500 mb lapse rate. It is most useful in determining thunderstorms due to orography, surface heating, and sea/lake breezes (Miller 1972). It is calculated by

$$VT = T_{850} - T_{500}, \quad (2)$$

where

T_{850} = temperature at 850 mb (°C)

T_{500} = temperature at 500 mb (°C)

Table 5 lists VT threshold values for North America and western Europe.

Table 5. Vertical Totals threshold values for North America and western Europe

| <i>VT threshold</i> | <i>Region</i> |
|---------------------|---|
| ≥30 | west coast of N. Amer., Great Lakes (unfrozen) |
| ≥28 | west of N. Amer. Continental Divide, western Europe |
| ≥26 | east of N. Amer. Continental Divide |
| ≥23 | Gulf of Mexico coastline, Gulf Stream |
| ≥22 | British Isles |

In mountainous regions, the sounding may have a high VT value, but the air mass cannot support thunderstorms unless there is also significant moisture. West of the North American Rocky Mountains, significant moisture is defined as:

- 700 mb or 500 mb dewpoint depression ≤ 6°C
- dewpoint temperature ≥ -17°C at 500 mb
- dewpoint temperature ≥ 0°C at 700 mb.

When significant moisture is present, the extent of thunderstorm activity in mountainous regions can be determined by the VT value, as listed in Table 6 (Air Weather Service 1979).

Table 6. Vertical Totals values and extent of thunderstorm activity in mountainous regions when significant moisture is present

| <i>VT Value</i> | <i>Thunderstorm extent</i> |
|-----------------|----------------------------|
| 28 | <3% of area |
| 29-32 | 4-15% of area |
| >32 | 16-45% of area |

2.4.5 Cross Totals

The Cross Totals (CT) measures low-level moisture and temperatures aloft (Miller 1972). It is not a good measure of instability in mountainous regions. It is calculated by

$$CT = T_{d850} - T_{500}, \quad (3)$$

where

$$\begin{aligned} T_{d850} &= 850 \text{ mb dew point temperature (}^{\circ}\text{C)} \\ T_{500} &= 500 \text{ mb temperature (}^{\circ}\text{C)} \end{aligned}$$

The CT threshold value for thunderstorms east of the North American Rocky Mountains is 18, except along the Gulf of Mexico coastline and over the Gulf Stream where the threshold value is 16.

2.4.6 Total Totals

The Total Totals (TT) is the sum of VT and CT. It is a more reliable predictor of severe weather activity in both warm- and cold-air situations than VT or CT alone. The TT must be used with attention to the amount of low-level moisture in the sounding, because large TT values due to high lapse rates may occur with little supporting low-level moisture (Air Weather Service 1979, Baker and Schlatter 1986). Table 7 lists the TT values and the corresponding thunderstorm activity for various regions of the United States.

Table 7. Total Total values and expected thunderstorm activity for United States

| <i>TT west of Rockies</i> | <i>TT east of Rockies</i> | <i>TT along Gulf Coast</i> | <i>Expected tstm activity</i> |
|---------------------------|---------------------------|----------------------------|-------------------------------|
| <48 | <44 | <39 | no convective activity |
| 48 to 51 | 44 to 45 | 39 to 40 | isol to few tstms |
| 52 to 54 | 46 to 47 | 41 to 42 | sct tstms |
| 55 to 57 | 48 to 49 | 43 to 44 | sct tstms, isol svr |
| 58 to 60 | 50 to 51 | 45 to 46 | sct tstms, few svr, isol tor |
| 61 to 63 | 52 to 55 | 47 to 50 | num tstms, sct svr, few tor |
| ≥ 64 | ≥ 56 | ≥ 51 | num tstms, sct svr, sct tor |

[NOTE: isol = <3% of area; few = 4-15% of area; sct = 16-45% of area; num = >45% of area; tstms = thunderstorms; svr = severe; tor = tornadoes]

2.4.7 Lid Strength

The *lid* (or *cap*) strength measures the strength of the capping inversion; that is, the ability of stable air aloft to inhibit low-level parcel ascent. In the absence of a lid, convection tends to be widespread but not intense. A strong lid may completely inhibit convection even in the presence of other thunderstorm indicators. If a lid is present but is broken late in the day, the convection along the lid boundary tends to become severe as the low-level heat and moisture quickly ascend to upper levels (Graziano and Carlson 1987, Hart and Korotky 1991).

The principal signature of the capping inversion is a relative humidity (RH) break. Criteria for identifying the break are:

- RH decreases with height by at least 1% mb⁻¹ between two successive significant levels not farther than 100 mb apart
- the upper of the two significant levels is 50 mb or more above the surface
- the base of the dry layer is below 500 mb.

If an RH break is present, the lower of the two significant levels is the level of the RH discontinuity. A capping inversion is present if it meets the following criteria:

- the sounding shows an increase in temperature or an isothermal layer within 100 mb above the level of RH discontinuity
- the lid base is the first significant level at the top of the isothermal or inversion layer
- the lid is below 500 mb.

If a lid is present, lid (LID) and buoyancy (BUOY) parameters are calculated:

$$LID = \theta_{sw1} - \bar{\theta}_w, \quad (4a)$$

and

$$BUOY = \theta_{sw5} - \bar{\theta}_w, \quad (4b)$$

where

- θ_{sw1} = maximum saturation wet bulb potential temperature in the inversion
- $\bar{\theta}_w$ = average wet bulb potential temperature in the 30-80 mb layer AGL
- θ_{sw5} = saturation wet bulb potential temperature at 500 mb

For $LID > 2$, DMC is unlikely in the absence of a strong source of lift. In unstable conditions ($BUOY \leq 1$), DMC is likely sometime during the day for $LID \leq 2$. If convection propagates into a region with $LID > 1.5$, the probability increases that the convection will become severe.

2.4.8 Buoyancy

Buoyancy measures the energy

- lost by a parcel rising adiabatically while it is colder than the surrounding environment (*convective inhibition*, or CIN);

- gained a parcel rising adiabatically while it is warmer than the surrounding environment (*convective available potential energy*, or CAPE).

CIN is a measure of the energy a parcel needs from a source of lift to reach its LFC. CAPE is another measure of latent instability. It has become favored over the traditional stability indices, such as LI, because CAPE is vertically integrated over the entire "positive region" of the sounding rather than calculated at mandatory levels (Weisman and Klemp 1982, Baker and Schlatter 1986, Hart and Korotky 1991, Doswell and Rasmussen 1994). The discussion as to the appropriate parcel to be lifted in Section 2.4.3 is valid here, because CAPE values are different with different lifted parcels.

2.4.8.1 Convective inhibition (CIN)

$$CIN = g \int_{z_{sfc}}^{z_{LFC}} \frac{T_v(z) - \bar{T}_v(z)}{\bar{T}_v(z)} dz, \quad (5)$$

where

- g = acceleration due to gravity
- z_{sfc} = surface level
- z_{LFC} = level of free convection
- $T_v(z)$ = parcel temperature using virtual temperature correction
- $\bar{T}_v(z)$ = sounding temperature using virtual temperature correction

For $CIN < -100$ J/kg, no free convection thunderstorms are expected.

2.4.8.2 Convective available potential energy (CAPE)

$$CAPE = g \int_{z_{LFC}}^{z_{EL}} \frac{T_v(z) - \bar{T}_v(z)}{\bar{T}_v(z)} dz, \quad (6)$$

where

- g = acceleration due to gravity
- z_{LFC} = level of free convection
- z_{EL} = equilibrium level
- $T_v(z)$ = parcel temperature using virtual temperature correction
- $\bar{T}_v(z)$ = sounding temperature using virtual temperature correction

The threshold values for the United States are:

- < 500 J/kg no thunderstorms
- 500 - 1500 J/kg thunderstorms
- > 1500 J/kg severe thunderstorms

Note that severe thunderstorms can occur with $CAPE < 1000$ J/kg, but the 0-3 km helicity must be greater than $300 \text{ m}^2/\text{s}^2$ (see Section 2.4.9).

2.4.9 Storm-relative environmental helicity

Storm-relative environmental helicity, or *helicity* for short, measures the streamwise vorticity (horizontal vorticity parallel to the horizontal wind flow) of the low-level wind profile. It has been found to be a good measure of the rotation potential that can be realized by a storm moving through a vertically sheared environment. Thus, it is used to determine if the environmental shear and the projected storm motion contain the potential for tornadic activity. Helicity can be visualized as minus twice the signed area swept out by the storm-relative wind vector in a layer on a hodograph diagram (Davies-Jones et al. 1990, Doswell 1991, Hart and Korotky 1991, Moller et al. 1994). It is calculated by

$$H = \sum_{n=0}^{N-1} [(u_{n+1} - c_x)(v_n - c_y) - (u_n - c_x)(v_{n+1} - c_y)], \quad (7)$$

where

- N = h , the depth of the inflow layer
(usually sfc-3 km AGL layer)
- (u_0, v_0) = surface wind
- $(u_1, v_1), \dots, (u_{N-1}, v_{N-1})$ = observed winds at successive levels between 0 and h
- (u_N, v_N) = interpolated wind at h
- (c_x, c_y) = storm motion horizontal wind components
 - = 20° to right and 85% of the 0-6 km mean wind vector for mean wind speed > 15 m/sec
 - = 30° to right and 75% of the 0-6 km mean wind vector for mean wind speed ≤ 15 m/sec (Johns et al. 1993)

Table 8 contains helicity values and the related tornado intensities that can be expected in the United States. It should be noted that the helicity values listed here are based on limited case studies and operational use; they can be expected to change as further data are collected.

Table 8. Helicity values and expected tornado intensities in United States

| <i>Helicity</i> (m^2/sec^2) | <i>Tornado intensity</i> (<i>Fujita damage scale</i>) | <i>Approximate wind speeds</i> |
|------------------------------------|--|--------------------------------|
| 100-299 | F0-F1 (weak) | 35-97 kts |
| 300-449 | F2-F3 (strong) | 98-179 kts |
| ≥ 450 | F4-F5 (violent) | ≥ 180 kts |

Helicity values are subject to rapid temporal and spatial changes and should be updated hourly when the potential for thunderstorms exists. In the absence of wind profiler data, a single-station forecaster should consider sending up a pibal to measure the boundary-layer winds when severe weather seems imminent.

2.5 Sources of Lift

Lifting is any process that supplies energy to a parcel to overcome the CIN ("negative area") of a sounding and bring the parcel to its LFC. Because convergence leads to upward motion, phenomena that produce low-level convergence are considered to be sources of lift.

2.5.1 Cold front

The *cold front* is an air mass boundary where warm air is replaced by cold air. Strong cyclonic wind shear and a pressure trough are often associated with a cold front. Strong surface convergence occurs in the frontal zone. Cold fronts are considered to be one of the best sources of lift, which has led some to designate thunderstorms as either frontal or non-frontal. The high values of vertical wind shear associated with vigorous cold fronts contribute to the formation of severe thunderstorms. Thunderstorms associated with cold fronts generally develop somewhat ahead of the front in the zone of strongest convergence.

2.5.2 Warm front

The *warm front* is an air mass boundary in which cold air is replaced by warm air. Even though warm fronts have cyclonic wind shear, a pressure trough, and convergence, these elements are usually weaker than those associated with cold fronts. The typical warm front has a shallower vertical slope compared to that of a cold front, leading to warm air aloft crossing over the frontal boundary and lying above the cold air mass (overrunning). Although warm fronts are less productive at lifting, the warm air and moisture behind the front can lead to rapid thermodynamic destabilization.

2.5.3 Dryline

The *dry line* is an area of intense moisture gradient separating dry desert air from moist maritime air. The 55°F isodrosotherm or 9 g kg⁻¹ isohume at the surface is considered to be the boundary between the air masses. It is typically located in a zone of small-scale convergence (Doswell 1982). The dryline often acts as a focus of convection, especially for severe thunderstorms (Schaefer 1986). Areas around the world where drylines are climatologically significant include the southern Great Plains of the United States, India in the premonsoon months, eastern China, and West Africa.

2.5.4 Outflow boundary from previous thunderstorm (mesoscale cold front)

One feature of the thunderstorm is the cold air downdraft. As this downdraft meets the surface, it spreads out laterally, forming what is known as a *gust front* or *outflow boundary*. The outflow boundary acts as a mesoscale cold front, with convergence, temperature contrasts on the order of 10°C km⁻¹, abrupt wind shifts, and pressure rises after passage. Moving away from the parent storm and into an unstable air mass, an outflow boundary can provide the source of lift needed to generate more thunderstorms (Doswell 1982).

2.5.5 Jet in vicinity

An area of large wind speeds confined to a narrow space is known as a *jet*. The presence of a jet suggests convergence in the region. In general, there are considered to be three levels where jets exist – low, middle, and high levels. The corresponding pressure levels are 850 mb, 500 mb, and 250 mb. The single-station forecaster usually will not have the spatial resolution to determine the extent of the jet. However, studies have established the critical jet speeds needed to differentiate between thunderstorm severity categories. Table 9 lists the jet heights, wind speeds, and expected thunderstorm severity in the United States when a jet acts as a source of lift.

Table 9. Jet heights, wind speeds, and expected thunderstorm severity in United States

| <i>Jet height</i> | <i>Sct tstms</i> | <i>Sct tstms, few svr</i> | <i>Num tstms, sct tor</i> |
|---------------------|------------------|---------------------------|---------------------------|
| 850 mb (low-level) | 20-25 kts | 25-35 kts | >35 kts |
| 500 mb (mid-level) | 30-35 kts | 35-50 kts | >50 kts |
| 250 mb (high-level) | 50-55 kts | 55-85 kts | >85 kts |

2.5.6 Topography

Topography plays a major role in creating localized areas of convergence and lifting. Although the circulations themselves can produce some weak thunderstorms, they may interact with other mesoscale or synoptic features that together provide a severe thunderstorm environment. The two best known topographic circulations are sea/land breezes and anabatic/katabatic flows.

2.5.6.1 Sea/land breezes

The *sea/land breeze* is a thermal circulation that develops when there is a large temperature gradient between a body of water and the adjoining land. The sea breeze occurs during the day and moves from the water to land; the land breeze occurs at night and moves from land to water. Both act as a mesoscale cold front. Convergence takes place at the "frontal" boundary between the water and land air.

An onshore wind helps to "push" the sea breeze front onshore and may, if the wind is strong enough, mask the presence of the front. In the case of an offshore wind, the sea breeze front may be prevented from moving onshore. In order to predict whether an offshore gradient wind (U) will prevent a sea breeze, the minimum temperature difference (ΔT_{\min}) between land and sea needed to initiate the sea breeze needs to be calculated (Walsh 1974):

$$\Delta T_{\min} = \frac{T_0}{0.11g} \left(\frac{\omega}{\kappa} \right)^{1/2} U^2, \quad (8)$$

where

| | | |
|-------------------|---|---|
| ΔT_{\min} | = | temperature _{land} - SST |
| T_0 | = | temperature (K) of land unaffected by water mass at initial time (usually the temp at 0600-0800 LST) |
| g | = | gravitational acceleration = 9.8 m sec ⁻² |
| ω | = | angular velocity of earth = 7.292×10^{-5} rad sec ⁻¹ |
| κ | = | eddy diffusion coefficient = 10 m ² sec ⁻¹ |
| U | = | gradient wind speed (m sec ⁻¹). |

When the predicted difference between max land temp and SST is greater than ΔT_{\min} , the sea breeze will move onshore.

2.5.6.2 Anabatic/katabatic flow

Anabatic and *katabatic* flows are thermal circulations generated by the temperature difference between a sloped surface and the free air. During the day, anabatic, or upslope, flow occurs because the sloped surface heats more quickly than the surrounding free air. Katabatic, or downslope, flow occurs at night because the sloped surface cools more quickly than the surrounding free air. Anabatic flow is enhanced on the windward sides of mountains; katabatic flow is only present on the lee sides of mountains because it is typically not strong enough to overcome the air flow on the windward sides. Convergence takes place at the boundary between the slope and free air.

Thunderstorms that develop due to anabatic flow often become detached from their originating circulation and move with the upper-level synoptic flow. As they reach the lee sides of the mountains, the upslope flow there can bring more warm air and moisture to the thunderstorms, triggering greater development. These are known as *lee slope* thunderstorms and can quickly become severe. However, when the mid-level steering wind, taken to be the 10,000-20,000 ft mean wind, has a component that blows up the climatological lee slope, no lee slope thunderstorms are expected because the weather is originating from a non-mountainous thunderstorm region. For example, if the climatological lee slope is the east side of a north/south-oriented mountain range, it will not have lee slope thunderstorms with wind directions from 000° through 180° (Henz 1972). The best known lee slope thunderstorms take place over the Great Plains of North America.

Besides anabatic flow, other topographic mechanisms that can initiate moist convection in the mountains include (Banta and Schaaf 1987):

- boundary-layer convergence, caused by the convergence of windward and leeward anabatic winds on the lee side
- updrafts induced by wake phenomena such as turbulence, gravity waves, and obstacle flow (split flow around the mountain)
- channeling into a convergent valley.

2.5.7 Differential advection

Differential advection is advection that occurs at some levels of the atmosphere but not at others. The types of advection that lead to convergence are warm advection at low levels (sfc

to 700 mb) or cold advection at middle or higher levels (at or above 500 mb). In the spring, differential advection separates convective from non-convective regions; in the summer, it separates severe from non-severe regions (Doswell 1982).

2.5.8 Detecting low-level convergence

There are times when the low-level convergence and the source of lift cannot be determined. However, significant low-level convergence can be detected by surface pressure falls greater than 1 mb/3 hr. The single-station forecaster must be prepared for changing weather in this event.

2.6 Assessing Severe Weather Potential

In his review of severe local storms, Ludlam (1963) pointed out that the vertical shear of the horizontal wind was an essential element for the formation and maintenance of most severe thunderstorms, given a favorable thermodynamic environment. Miller's (1972) five synoptic patterns conducive for tornadic storms qualitatively recognized vertical wind shear.

Quantitative methods for operationally determining vertical wind shear have been slow to develop, as compared to stability indices. The SWEAT Index used by the Air Force includes a term to estimate the vertical wind shear (Air Weather Service 1979). Recently, other indices combining thermodynamics and vertical wind shear have been developed. In addition, attention has been renewed in hodograph analysis as a means of locating areas of vertical wind shear (Doswell 1991). For example, the SHARP Workstation currently used by the National Weather Service includes both sounding analysis and hodograph analysis routines (Hart and Korotky 1991). For the single-station forecaster, surface winds backing with time and increasing in speed denote the development of vertical wind shear favorable for a severe storm environment.

It needs to be stressed that a *combination* of favorable thermodynamics and wind shear is necessary for severe storm development. Note that severe storms can occur with low instability or low vertical wind shear, but the corresponding wind shear or instability must be very strong in order to overcome the unfavorable environment.

2.6.1 SWEAT Index

The SWEAT (Severe WEAther Threat) Index estimates the severe weather potential of a given air mass. It is best used with a daytime sounding. It is calculated by

$$\text{SWEAT} = 12T_{d850} + 20(\text{TT} - 49) + 2U_{850} + U_{500} + 125(S + 0.2), \quad (9)$$

where

| | | |
|------------|---|--|
| T_{d850} | = | 850 mb dew point temperature (°C) |
| TT | = | Total Totals Index (Section 2.4.6) |
| U_{850} | = | 850 mb wind speed (kts) |
| U_{500} | = | 500 mb wind speed (kts) |
| S | = | $\sin [(500 \text{ mb wind direction}) - (850 \text{ mb wind direction})]$ |

The shear term $[125(S+0.2)]$ is set to zero when any of the following conditions are *not* met:

- 850 mb wind direction is from 130° through 250°
- 500 mb wind direction is from 210° through 310°
- $[(500 \text{ mb wind direction}) - (850 \text{ mb wind direction})] > 0$
- 850 mb and 500 mb wind speeds are both greater than or equal to 15 kts

The threshold values for the United States are:

- ≥ 300 severe thunderstorms
- ≥ 400 tornadoes

For stations above 850 mb, the temperature, dewpoint, and winds at 100 mb above ground level are used in place of 850 mb parameters. Note that no term in the formula may be negative.

2.6.2 Bulk Richardson Number

The Bulk Richardson Number (BRN) is a combination of instability and the vertical wind shear from the surface to 6 km height. It predicts whether storm cells will be supercellular (*mesocyclone*) or multicellular (*squall line*) (Weisman and Klemp 1982, 1984, 1986). Approximately 50% of mesocyclones develop tornadoes (Brooks et al. 1994). The BRN is calculated by:

$$\text{BRN} = \frac{\text{CAPE}}{\frac{1}{2} \left[(u_{0-6} - u_{sfc})^2 + (v_{0-6} - v_{sfc})^2 \right]}, \quad (10)$$

where

- CAPE = convective available potential energy (Section 2.4.8.2)
- u_{0-6}, v_{0-6} = density-weighted mean wind speed components over a 6 km depth
- u_{sfc}, v_{sfc} = surface layer wind speed components (lowest 500 m)

The critical BRN values for the United States are:

- 8-40 "classic" isolated supercells
- >50 multicells

for CAPE in the range 1500-3500 J/kg.

When the denominator of BRN, called BRN shear, is less than $3 \times 10^{-3} \text{ s}^{-1}$, the shear will be too weak to provide substantial organization to the convection. Vertical wind shear is the more important parameter in determining whether supercell development will occur.

Supercells have been observed within complex convective structures, such as cold sector thunderstorms, with BRN less than 14 due to low CAPE ($<1000 \text{ J/kg}$) and/or high shear. In these cases, helicity (Section 2.4.9) should be calculated to determine whether the low-level shear will be favorable for the development of a rotating updraft (Monteverdi and Quadros 1994).

2.6.3 Energy-Helicity Index

The Energy-Helicity Index (EHI) measures the combination of CAPE and helicity needed to produce severe thunderstorms. It is calculated by

$$EHI = CAPE \times \frac{H}{160000}, \quad (11)$$

where

CAPE = convective available potential energy (Section 2.4.8.2)
H = helicity (Section 2.4.9)

The threshold values for the United States are:

- EHI ≥ 0.5 weak severe thunderstorms (F1) (Monteverdi and Quadros 1994)
- EHI > 1 strong severe thunderstorms (F2-F3) (Brooks et al. 1994)
- EHI > 2.5 violent severe thunderstorms (F4-F5) (Brooks et al. 1994)

Brooks et al. (1994) noted that EHI does a good job of defining environments capable of supporting mesocyclones, but does not discriminate well between tornadic and non-tornadic mesocyclones.

2.6.4 Storm Severity Index

The Storm Severity Index (SSI) is another way to determine the combination of instability and vertical wind shear needed to produce severe thunderstorms (Turcotte and Vigneux 1987). It is calculated by

$$SSI = 100[2 + (0.276 \times \ln(Shr)) + ((2.011 \times 10^{-4}) \times CAPE)], \quad (12)$$

where

Shr = mean wind shear from surface to 12,000 ft (~4 km)
CAPE = convective available potential energy (Section 2.4.8.2)

For SSI ≥ 100 , severe thunderstorms can be expected.

3. FOG AND STRATUS

3.1 Introduction

Fog and low stratus are clouds that form at or near the surface of the earth (Air Weather Service 1954). Distinguishing between fog and stratus depends on one's location; what is stratus to a person in a valley is fog to someone else at a higher elevation. Fog is the most frequent cause of ground visibilities going below three miles (FAA and Dept. of Commerce 1965). Fog and stratus can also lower ceilings below flight minimums. Because fog and low stratus are near-surface phenomena, they are a hazard to aviation primarily on takeoffs and landings.

Fog and stratus develop when an air mass becomes saturated. Air can be brought to saturation by any of three processes – cooling, addition of water vapor, or mixing with another air mass. Cooling occurs with one or more of the following processes:

- outgoing long-wave radiation and resultant cooling of the near-surface air
- advection of air over a colder surface
- adiabatic cooling by orographic, frontal, or turbulent lifting
- evaporative cooling by falling precipitation.

Addition of water vapor occurs with one or more of the following processes:

- evaporation from falling precipitation
- evaporation from a wet surface
- moisture released during combustion of hydrocarbon fuels
- turbulent transfer of moisture.

The mixing of two nearly saturated air masses at different temperatures can also result in saturation.

Fog and stratus dissipation occurs with either of two processes – heating of the air or removal of water vapor. Heating can be caused by

- incoming short-wave radiation and resultant warming of the near-surface layer
- advection over a warmer surface
- adiabatic warming by subsidence, downslope motion, or turbulent transfer downward
- turbulent mixing with warmer air.

Water vapor is removed by

- turbulent transfer of moisture upward
- turbulent mixing with drier air
- condensation of water vapor in the form of dew or frost.

Fog can be divided into three categories – radiation, advection, and frontal. *Radiation fog* forms when air is cooled to the dew point through long-wave radiative cooling. *Advection fog* develops when a warm moist air mass is advected over a cooler surface or is lifted adiabatically, lowering the temperature of the air mass to the dew point. *Frontal fog* occurs near the boundaries of warm and cold fronts where mixing of the two air masses occurs. In addition, radiative cooling enhances the formation of advection or frontal fog.

Radiation fog can form anywhere in the world when the conditions are right. Advection fog, on the other hand, needs a source of warm moist air and favorable synoptic conditions, so it tends to form in regions with maritime climates and on the windward sides of mountains. Figures 5 through 8 show the percentage frequency of fog during January, April, July, and October, respectively, for the world (Guttman 1971). It is seen that the greatest frequency of fog occurs mostly along coastlines. The polar regions (poleward of 60°) have a high fog frequency due to cold temperatures and warm air advection poleward. Areas with large concentrations of condensation nuclei, such as industrial regions and coastlines affected by dust storms, are also more prone to fog.

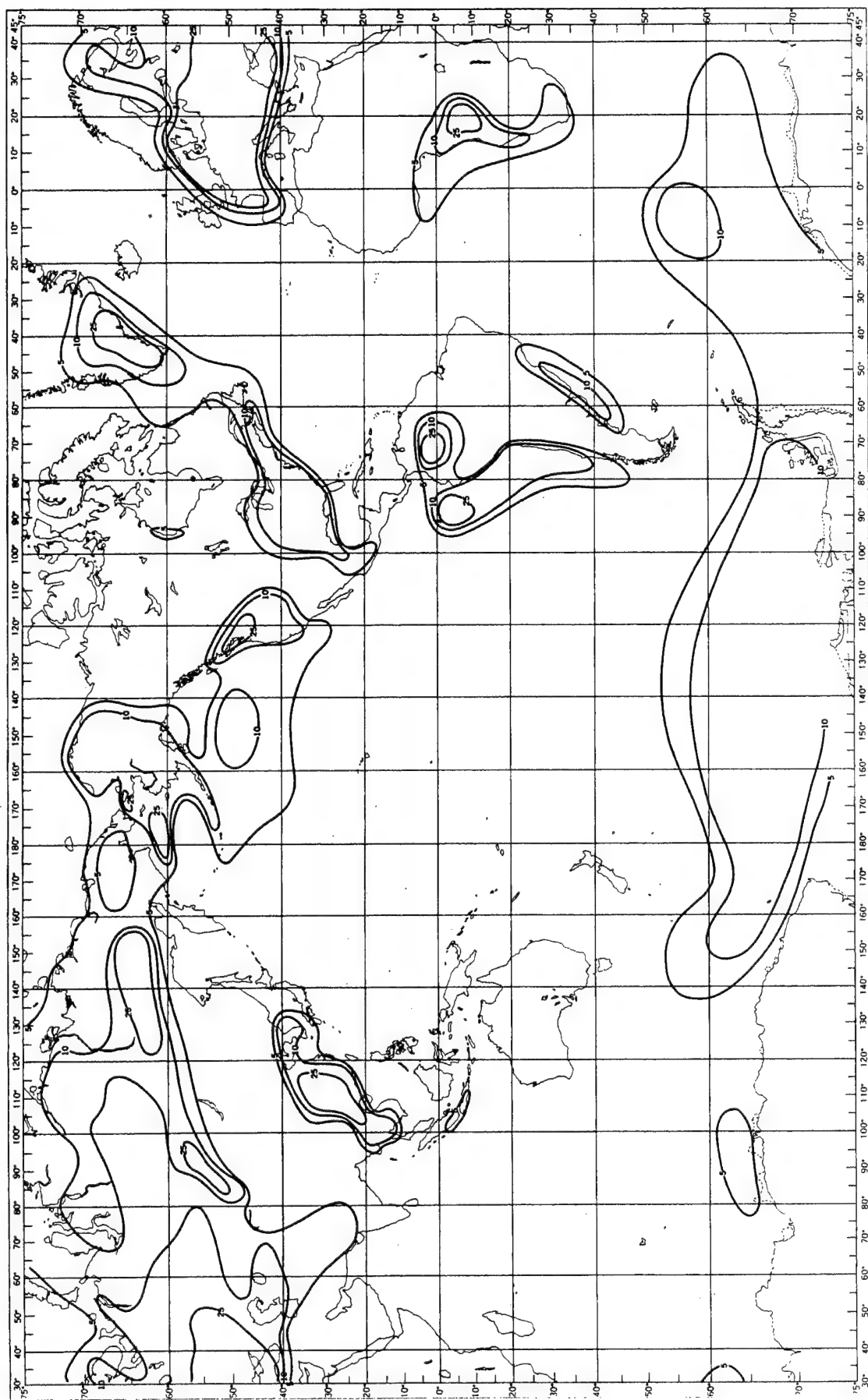


Figure 5. Percentage frequency of occurrence of fog, January (From Guttman 1971)

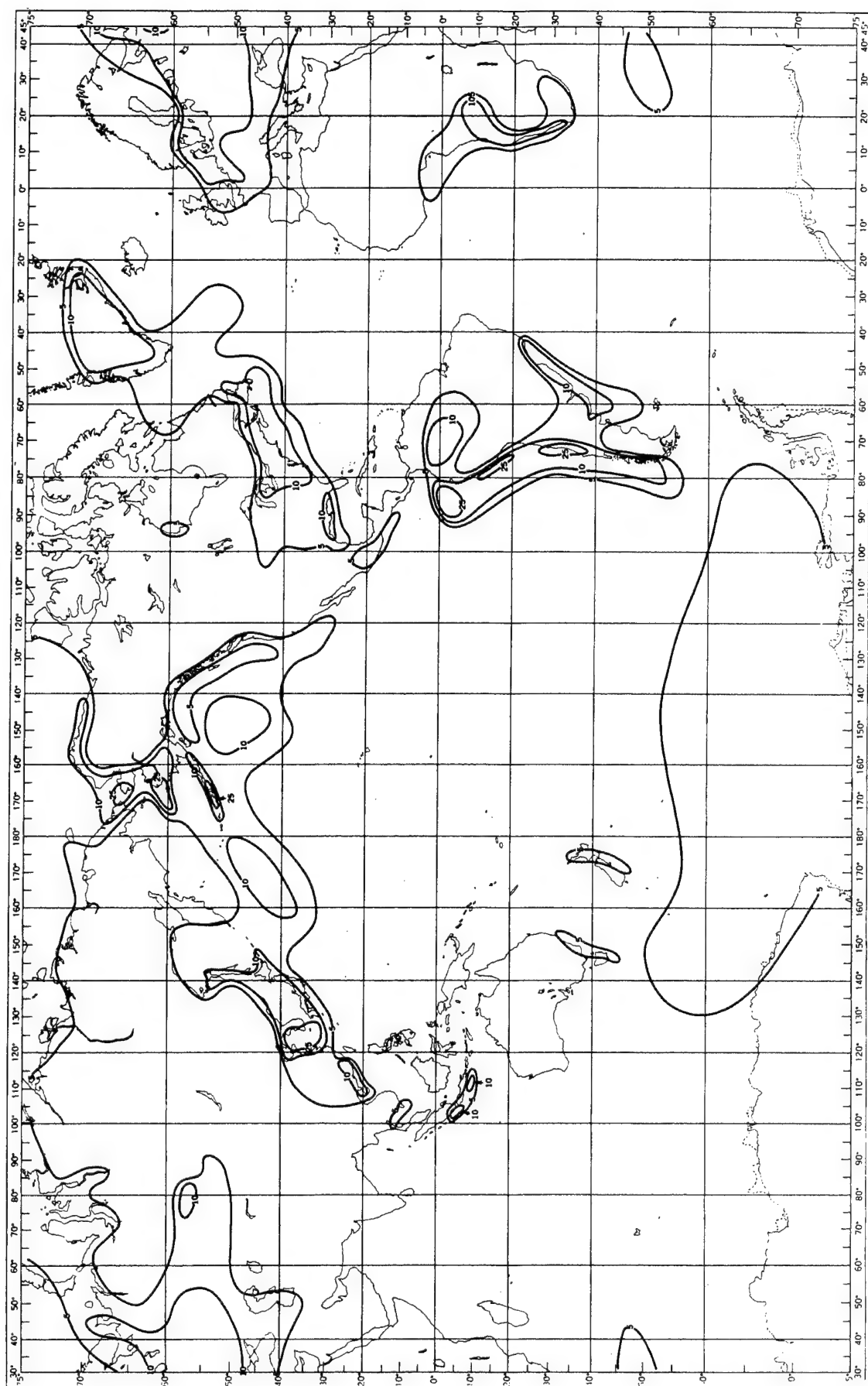


Figure 6. Percentage frequency of occurrence of fog, April (From Guttman 1971)

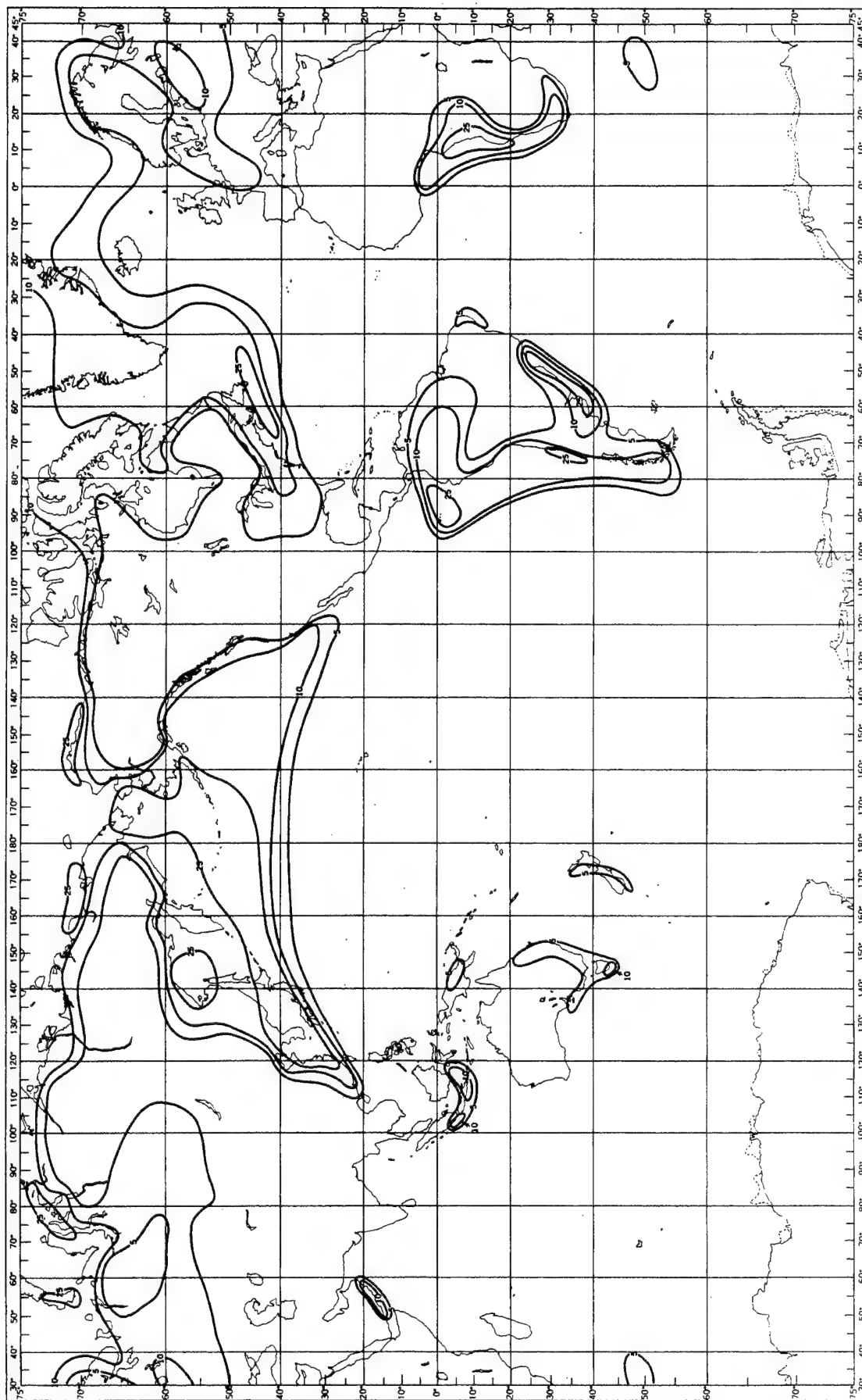


Figure 7. Percentage frequency of occurrence of fog, July (From Guttman 1971)

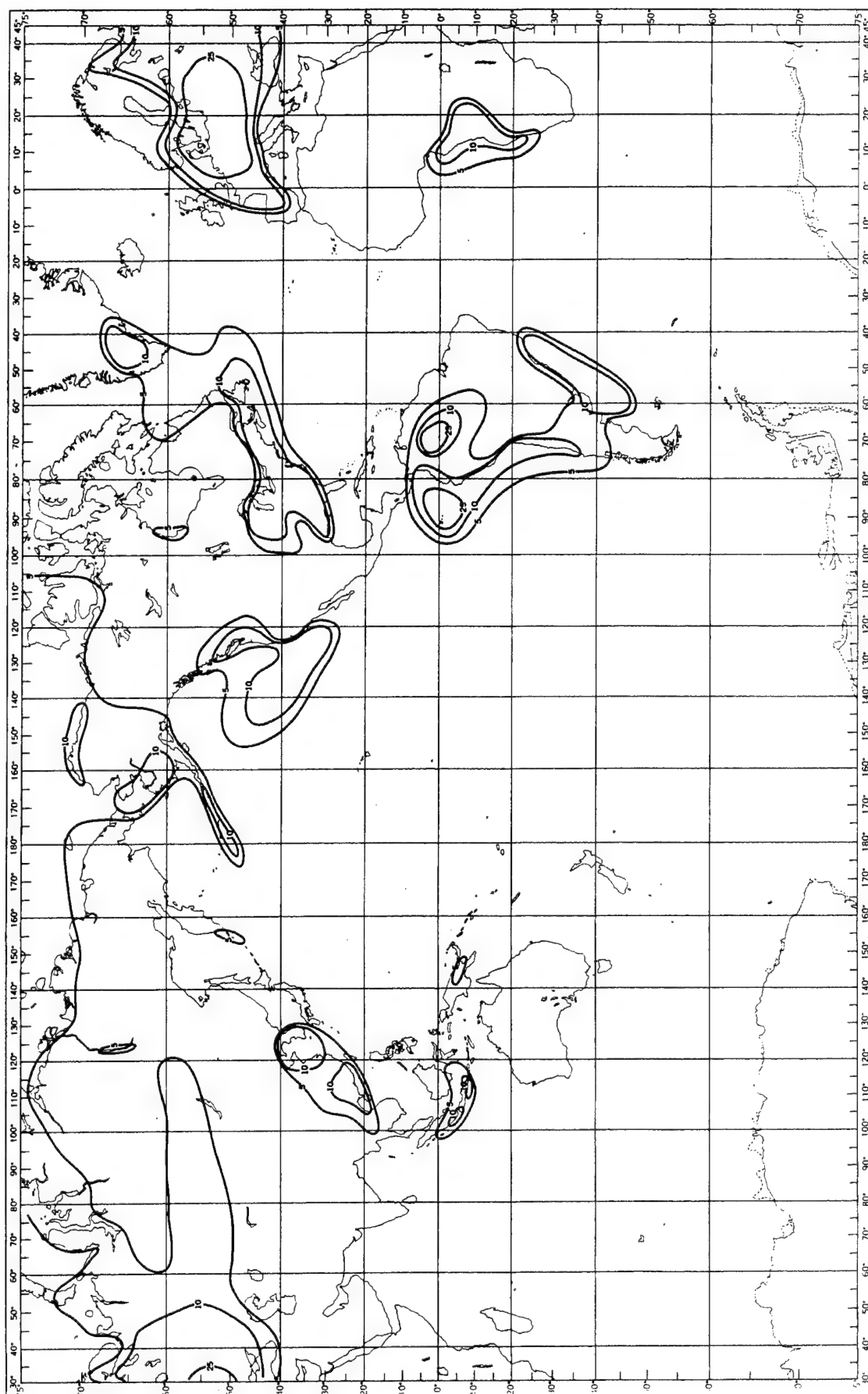


Figure 8. Percentage frequency of occurrence of fog, October (From Guttman 1971)

3.2 Radiation Fogs

Radiation fogs are divided into two types – those associated with a surface-based inversion, called *ground fog*, and those associated with an inversion based above the surface, called *continental high-inversion fog*.

3.2.1 Ground fog

The favored locations for ground fog are mountain and river valleys, wide flat plains, marshy areas, and tropical rainforests. Ground fog can occur anywhere in the world given the right conditions. The highest frequency of ground fog worldwide occurs in:

- western half Amazon River basin; year-round
- Congo River basin; year-round
- southern Yunnan Province of China and northern Indochina; October through March

The usual synoptic situation for ground fog formation is a high pressure center or ridge. In the mid-latitudes a cold frontal passage 24-48 hours earlier generally precedes the high pressure. In the Tropics rainfall during the previous day is a forecast indicator of fog. The sky cover must be clear; even a thin layer of cirrus will retard outgoing long-wave radiation. The surface winds should be light, usually less than 2 m sec^{-1} (5 kts). The vertical profile is a surface-based inversion with moist air in the inversion and dry air aloft. Dissipation is through insolation; the majority of fogs dissipate within three hours after sunrise.

Ground fog has a tendency to intensify the first hour after sunrise during the transition from the nocturnal cooling process to the daytime boundary layer mixing process. Some fogs develop shortly after sunrise when saturation is reached due to evaporation of dew (Pilié et al. 1975).

3.2.2 Continental high-inversion fog

Continental high-inversion fog is a winter radiation fog that has an inversion based above the surface. The favored regions are broad valleys and basins with access to maritime air. The worldwide locations and preferred time of year are:

- North American Pacific coast valleys, especially Puget Sound, Willamette River, and San Joaquin Valleys; October through February
- South American Pacific coast valleys, especially Central Valley of Chile; year-round, maximum May through August.
- European river valleys; year-round, maximum November through March
- Gulf of Guinea region; November through May
- Sichuan Basin and greater Yangtze River valley; year-round, maximum November through March
- southeast Australia, Tasmania, and New Zealand coastal valleys; May through September

The usual synoptic situation for fog formation is cool moist air trapped in a valley by stagnant high pressure. A forecast indicator is precipitation within the last 24 hours. The sky cover is usually cloudy through the day, restricting heating at the surface, and then clearing at sunset for maximum long-wave radiation. The surface winds should be less than 4 m sec^{-1} (8 kts). The vertical profile is a subsidence inversion with the base above the surface. Dissipation is through insolation or a synoptic weather change.

During a persistent fog regime, the fog will lift to a stratus deck during the day and return at sunset; eventually the fog will remain all day due to the lack of solar heating at the ground and the continued radiational cooling at the top of the stratus/fog deck. Only a synoptic weather change that replaces the maritime air in the valleys will break the regime.

3.3 Advection Fogs

3.3.1 Marine high-inversion stratus/fog

Marine high-inversion stratus/fog is stratus that forms over a cold coastal current and is advected onshore. Fog occasionally forms under the inversion if the air mass is moist enough. The favored regions are coastlines with upwelling or cold water currents. The worldwide locations and preferred time of year are:

- Pacific coastline of North America from Vancouver Island through Baja California; year-round, maximum June-August (*California stratus*)
- Pacific coastline of South America south of 3°S ; year-round, maximum March-July (*camanchaca*) (Gilford et al. 1992)
- coastlines of northern and central Europe; April through October
- North Atlantic coastline of Africa; year-round, maximum June-August
- South Atlantic coastline of Africa; year-round, maximum June-September (*cacimbo*) (Traxler et al. 1994)
- Gulf of Guinea region; June through September
- Horn of Africa and eastern coastline of Arabian Peninsula; June through September
- southern Indonesia; April through October

The usual synoptic situation has the region in the subsiding air of a subtropical high or heat low and a weak synoptic pressure gradient. The air mass has a trajectory first over warm water, then over upwelled water, and is finally advected onshore by the sea breeze or by the general circulation in the region. Forecast indicators are clear skies, light offshore flow, and the upwelled sea surface temperatures colder than the air temperature at the station. During a stratus/fog regime, the sky cover is marine stratus with no middle or high clouds, and onshore surface winds. The vertical profile is a subsidence inversion with its base greater than 400 m above the surface, and a turbulent mixed layer below the inversion. Dissipation is through insolation or a synoptic weather change.

The stratus/fog forms at night below the stratus deck and is advected inland during the day. The lower the base of the subsidence inversion, the more likely the stratus/fog will form. The

stratus regime may last for several days, with each day seeing the stratus/fog developing earlier and dissipating later. The regime is usually broken with a frontal passage.

3.3.2 Coastal high-inversion stratus/fog, continental origin

The coastal high-inversion stratus/fog of continental origin, known as the *surge* or the *marine push*, is a special case of the marine high-inversion fog. It develops when a heat low expands and keeps marine air from coming onshore. When the heat low retreats, the marine air that had been dammed up surges onshore, acting like a mesoscale cold front. The worst ceilings and visibilities occur within the 24 hours after the surge begins, then gradually improve (Mass et al. 1986, Mass and Albright 1987, Jannuzzi 1993, Felsch and Whitlatch 1993).

Favored regions are mountainous coastlines with cold water currents. The worldwide locations and preferred time of year are:

- Pacific Northwest; May through September
- southern California; September through March
- southern coastline of Africa from southern Namibia through eastern South Africa; May through September

The usual synoptic situation is a thermal low or high pressure inland and a cold front offshore. Signs that the thermal low has expanded include clear skies, offshore flow, high temperatures and low humidity, and no inversion near the surface. The surge begins when offshore flow suddenly reverses to onshore, pressure and humidity rise, and temperatures fall. Marine stratus and fog are advected onshore. The surface winds become onshore, strong and gusty, and ageostrophic. The vertical profile is similar to the marine high-inversion stratus/fog case, with a low inversion base above the surface, beginning at about 200 m and slowly rising with time, and a turbulent mixed layer below the inversion. Dissipation is through insolation or synoptic weather change.

In general, the greater the warm air anomaly and the longer the offshore wind lasts, the stronger the surge will be when it arrives (Jannuzzi 1997). The difference between the sea surface temperature and the warm air, not the time of day, is critical for fog formation and advection. Leipper (1995) stated that a sea surface-air temperature difference of at least 5°C is a good precursor of fog.

In Africa the offshore wind is called a *berg* wind, the onshore wind is called a *buster* wind, and the mesoscale cold front is called a *leader front* (Reason and Jury 1990, Traxler et al. 1994). In southern California the offshore wind is called a *Santa Ana*. The fog that affects southern California after a Santa Ana is much denser than the fog that forms in conjunction with California stratus (Noonkester 1979, Leipper 1994).

3.3.3 Sea fog

Sea fog develops when a poleward-traveling air mass passes over a warm current and then a cold current. Over the warm current the air mass expands and becomes moister. Over the cold current the air mass is quickly cooled to the dew point. Sea fog is a problem at the

coastlines near the cold currents, because the fog can be quite dense and it is not dissipated by insolation.

Favored regions for sea fog are at the conjunction of warm and cold water currents. The worldwide locations and preferred times of year are:

- North American coastline from Newfoundland to Cape Cod; year-round, maximum June-August [conjunction of Labrador Current (cold) and Gulf Stream (warm)]
- northeastern Asian coastline; year-round, maximum June to July [conjunction of Oyashio Current (cold) and Kuroshio Current (warm)]
- Galapagos Islands; year-round [conjunction of Peru Current (cold) and Equatorial Counter Current (warm)]
- polar waters of both hemispheres; summer half-season

The usual synoptic situation is air with a trajectory first over warm water, then over cold water, that is finally advected onshore. The air and dewpoint temperatures will be equal to the sea surface temperature at the time of fog formation. Forecast indicators for sea fog are a large temperature difference between the air (warm) and the sea surface temperature (cold), and the dewpoint temperature of the air warmer than the sea surface temperature. Sky cover and radiative effects are not a factor because of the pure advective nature of the fog. The surface winds on the land are onshore, but wind speed is not a factor. The vertical profile is a strong surface-based inversion. Sea fog quickly dissipates inland because the land temperature is usually warmer than the air temperature; coastlines are the most affected land areas. Dissipation occurs when a synoptic weather change reverses the direction of the air trajectory.

Sea fog is the most persistent kind of fog because sea surface temperatures are not affected by the diurnal change in air temperature. If the initial dewpoint temperature of the air is less than the cold-current sea surface temperature, fog formation is unlikely.

3.3.4 Advection-Radiation Fog

Advection-radiation fog is a fog that depends on both advective and radiative effects for formation. Air over warm coastal waters is advected onshore during the day and then cooled to the dew point during nighttime radiative cooling. Favored regions are coastal areas open to tropical maritime air, and coastlines of large lakes and inland seas with water temperatures colder than the overlying air. The worldwide locations and preferred time of year are:

- North Atlantic coastline south of Cape Cod and Gulf of Mexico coastline of United States; September through February
- Great Lakes coastline; April-June
- Europe; November through March
- South China and northern Indochina coastline; January through April (*crachin*) (Huschke 1959)
- Korea and East China coastlines; year-round, maximum May through August

The usual synoptic situation for fog formation is onshore flow, falling air temperatures, rising dewpoint temperatures, and the ground or lake surface temperature initially colder than the advected air temperature. [For crachin development, the maritime air is initially cooled by passage over a coastal belt of cold water rather than the ground (Ramage 1954, 1971).]

When the air temperature falls to within a degree of the ground or cold water temperature, fog begins to form. Forecast indicators are some cloudiness and/or cold advection over land during the daytime, and an air trajectory over warm seas and then over cold land or water. At the time of fog formation, the sky cover is a layer of stratus below the turbulence inversion that builds downward as the moisture content of the onshore air increases. The surface winds are light onshore. The vertical profile is warm moist air at surface capped by a turbulence inversion. Dissipation is through insolation or a synoptic weather change.

Advection-radiation fog will not develop with the following conditions (Air Weather Service 1954):

- insufficient moisture in the advected air
- air over land significantly warmed by solar heating the previous day
- insufficient nocturnal radiational cooling due to a low cloud cover
- insufficient advective cooling due to a weak temperature gradient
- high wind speed causing turbulence in lower layers and higher cloud bases
- adiabatic warming due to downslope air motion
- advection blocked by mountains.

3.4 Frontal Fogs

Frontal fogs develop when the stable air in the cold sector of the front becomes saturated due to precipitation falling into it (Byers 1959). Most frontal fogs are associated with warm fronts, although shallow cold fronts with stable air behind them may also develop fog. Stations on the windward side of sloped terrain develop fog more quickly than stations at lower elevations because of the added contribution of adiabatic cooling (George 1951). Frontal fogs are most prevalent in the winter season, when the contrast between air masses is greatest.

3.4.1 Warm fronts

The favored regions for warm frontal fog are areas with well-developed warm fronts during the winter season. The worldwide locations and preferred time of year are:

- eastern half of United States; November through March
- Europe; November through March

The usual synoptic situation has the station in the cold sector of a strong warm or stationary front, active upgliding or uplifting of warm air over the frontal surface (overrunning), and precipitation into the cold air bringing the surface air to saturation. Before the approach of the warm front, the region usually has been under the influence of continental polar air. At the time of fog formation, the sky cover is stratus or nimbostratus, and the surface wind speeds are low. The vertical profile shows cold stable air below the frontal surface and warm

moist air above the frontal surface, with the cloud base temperature warmer than the surface air temperature. Dissipation is usually through a synoptic weather change, although a pre-warm front fog in late spring may be dissipated by insolation.

Dense fog can occur when the cold sector air temperature is a few degrees above freezing and lies over snow cover. The combination of melting snow at the surface and strong warm air advection leads to supersaturation and widespread fog (Petterssen 1956).

3.4.2 Cold fronts

The favored regions for cold frontal fog are areas where tropical air overlies a shallow polar air layer behind an east/west-oriented cold front. The worldwide locations and preferred time of year are:

- Great Plains of North America; September through April (*Cheyenne fog*) (Byers 1959)
- eastern South America coastline from southern Brazil to northern Argentina; year-round, maximum June through August (*sudestada*) (Gilford et al. 1992)
- Gulf of Tonkin coastline; January through April

The usual synoptic situation has the station in the cold sector of the cold front with the cold air sliding under the warm air lying over the frontal surface, and precipitation into the cold air bringing the surface air to saturation. Before the cold front passage, the warm-sector precipitation brings the air at the station close to saturation. At the time of fog formation, the sky cover is stratus or nimbostratus. The surface wind speeds are usually low, but cases have been recorded of dense surface fogs with wind speeds of 20 to 30 mph (Byers 1959). The vertical profile shows cold stable air below the frontal surface and warm moist air above the frontal surface, with the cloud base temperature warmer than the surface air temperature. Dissipation is through a synoptic weather change.

In the Great Plains, Cheyenne fog has also been called *upslope fog*, because cooling of the air through adiabatic expansion as it traveled from east to west had been thought to play the primary role. However, George (1951) stated that precipitation before and during the fog is the primary way the air reaches saturation, although adiabatic cooling may be a contributing factor.

3.5 Fog Forecasting Methods

Many stations have developed conditional climatologies, objective studies, and fog curves (for example, see Naistat 1988) for forecasting fog formation and dissipation. Advection fog forecasting requires a knowledge of the synoptic situation. Radiation fog formation, on the other hand, is a local process. This makes radiation fog both easier and more difficult to forecast. It is easier in that the forecaster only has to monitor the local observations. It is more difficult in that the forecaster needs to know how topography affects wind flow around the station, where the local sources of moisture are, and the local climatology. The following forecast methods for fog formation are to be used to determine the possibility of fog formation through radiative cooling *only*. The fog dissipation methods can be used for both

advection and radiation fogs because insolation is the primary way fog is dissipated over land.

3.5.1 Radiation fog formation

The ideal conditions for radiation fog formation are a stable moist air mass, clear skies, and light winds. If these conditions are met, the following indices and model can be used to assess the potential of the atmosphere to reach saturation.

3.5.1.1 Fog Stability Index

The Fog Stability Index (FSI) assesses the chance of radiation fog development. It is calculated by

$$FSI = 4T_{sfc} - 2(T_{850} + Td_{sfc}) + W_{850}, \quad (13)$$

where

- T_{sfc} = surface temperature ($^{\circ}\text{C}$)
- T_{850} = 850 mb temperature ($^{\circ}\text{C}$)
- Td_{sfc} = surface dew point temperature ($^{\circ}\text{C}$)
- W_{850} = 850 mb wind speed (kts)

using values from the evening sounding. Table 10 lists the values of FSI and the corresponding chances of radiation fog (Air Weather Service 1979).

Table 10. Fog Stability Index values and the likelihood of radiation fog

| <i>FSI</i> | <i>Likelihood of radiation fog</i> |
|------------|------------------------------------|
| >55 | low |
| 31-55 | moderate |
| <31 | high |

3.5.1.2 Fog Point Temperature

Fog point temperature (T_f) is the temperature at which radiation fog will form. It is determined from the evening sounding plotted on an adiabatic chart using the following steps:

- Determine the LCL.
- Determine the saturation mixing ratio at the point where the dewpoint temperature profile crosses the LCL.
- Follow the saturation mixing ratio line from the LCL to the surface. The temperature at this point is the fog point temperature T_f .

If the low temperature is forecast to be less than T_f , radiation fog can be expected to form (Air Weather Service 1979).

3.5.1.3 Fog Threat Index

The Fog Threat (FT) Index measures the degree of the threat of fog formation by radiational cooling. It is calculated by

$$FT = \theta_{w850} - T_f, \quad (14)$$

where

$$\begin{aligned} \theta_{w850} &= 850 \text{ mb wet bulb potential temperature} \\ T_f &= \text{fog point temperature (Section 3.2.1.2)} \end{aligned}$$

Table 11 lists the Fog Threat values and the corresponding chances of radiation fog (Air Weather Service 1979).

Table 11. Fog Threat values and the likelihood of radiation fog

| <i>Fog Threat</i> | <i>Likelihood of radiation fog</i> |
|-------------------|------------------------------------|
| >3 | low |
| 0-3 | moderate |
| <0 | high |

3.5.1.4 Ground fog model

A model for ground fog formation has been developed by Meyer and Lala (1990). It determines the time (τ) for the near-surface atmosphere to reach saturation; τ is compared to the length of night (LON) to see if the night is long enough for saturation to be reached by radiational cooling. The time τ is calculated by

$$\tau = \frac{\frac{R_d T^2}{\epsilon L_v} \ln(RH_0)}{\frac{\partial T}{\partial t}}, \quad (15)$$

where

$$\begin{aligned} \tau &= \text{time to reach saturation after sunset (hr)} \\ R_d &= \text{gas constant for dry air} \\ T &= \text{temperature at sunset (K)} \\ \epsilon &= R_d/R_v \\ R_v &= \text{gas constant for water vapor} \\ L_v &= \text{latent heat of vaporization} \\ RH_0 &= \text{relative humidity at sunset} \\ \frac{\partial T}{\partial t} &= \text{nighttime cooling rate (deg hr}^{-1}\text{)} \end{aligned}$$

If $\tau < \text{LON}$, radiation fog is probable. The time of formation will be $\tau + \text{sunset time}$. If [(time of sunrise) - (time of formation)] is greater than 2 hours, there is a higher probability of severe fog, defined as visibility less than 100 m. If the surface temperature and dewpoint

temperature begin increasing during the night, fog can be expected to form in about an hour. If $\tau > \text{LON}$, radiation fog is not likely because sunrise will occur before the atmosphere reaches saturation.

The critical parameters for forecasting the onset time of ground fog are the initial relative humidity and the cooling rate. The cooling rate for clear skies and non-snow-covered ground is $0.6\text{--}1.0^\circ\text{C hr}^{-1}$ (Pilié et al. 1975, Fitzjarrald and Lala 1989, Meyer and Lala 1990). Under clear-sky conditions the nocturnal cooling rate is usually constant.

Comparisons between the predicted time of fog formation and the observed time of fog formation show that fog developed within two hours of the predicted time over 60% of the time. However, this model errs in forecasting fog too often. Meyer and Lala (1990) found that τ forecasted less than half of the no-fog conditions out of 27 cases. On the other hand, τ only once predicted a no-fog condition for a night that had observed fog.

3.5.2 Fog and stratus dissipation by insolation

Insolation is the primary way both radiation and advection fogs are dissipated. However, the possibility of fog re-formation must be considered every evening the stable and/or advective regime continues. The following methods determine the critical temperature (T_c) at the surface required to dissipate the fog layer and the time when the fog layer will dissipate (Air Weather Service 1954).

3.5.2.1 Raob method

On an adiabatic chart, plot the morning sounding. Mark the height of the ceiling (from surface observations) on the sounding – this is the base of the fog layer. Determine the mixing ratio at the point where the sounding intersects the fog base. Continue this mixing ratio line upward until it intersects the sounding in the inversion. Draw a dry adiabat from this point to the surface. The temperature at the surface is the temperature T_c .

3.5.2.2 Fletcher method

On an adiabatic chart, plot the morning sounding. Mark the height of the ceiling (from surface observations) on the sounding – this is the base of the fog layer. Mark the height of the inversion base on the sounding – this is the top of the fog layer. Determine the thickness of the fog layer (Δh) by subtracting the height of the fog layer base from the height of the fog layer top. The fog dissipation temperature T_c is calculated by

$$T_c = T_{sfc} + \frac{\Delta h}{210}, \quad (16)$$

where

- T_{sfc} = present surface temperature ($^\circ\text{F}$)
- Δh = thickness of fog layer (ft)
- 210 = empirical number; each 1°F of surface temperature rise will lift the ceiling 210 ft ($\text{ft}/^\circ\text{F}$)

3.5.2.3 Determine time of fog dissipation.

Determine T_c by one of the above methods. Construct a diurnal temperature curve for the station by using the observed sunrise temperature and forecasting the clear-sky maximum temperature (T_m) from solar heating tables (for example, Table 134 in List 1963) or climatology. Correct the curve in order to take the lack of solar insolation at the surface into account (T_a); McGinley (1986) suggested a factor of 0.5 for overcast skies. The time when $T_a = T_c$ is the time of fog dissipation. If $T_a = T_c$ occurs after T_m is expected, or if T_c is greater than T_m , the fog will not dissipate.

4. WINTER PRECIPITATION

4.1 Introduction

Winter precipitation, or precipitation that is frozen in some way, is another hazard to aviation operations. On the ground, accumulated snow needs to be removed, scraped surfaces remain slippery, aircraft deicing must be done before takeoff, and cold temperatures make outdoor work difficult. During takeoffs and landings there is also the danger of icing from supercooled water droplets, changing aircraft aerodynamics due to snow loading, low visibilities during snowfall, and sliding off the runway.

Once a single-station forecaster realizes that a winter storm will impact the station, the major forecast problems become predicting the type of precipitation that will fall and the accumulation of frozen precipitation. This section will outline means to determine the rain/snow line, ways to determine when freezing rain and ice pellets (sleet) will fall, and some methods for forecasting snow accumulation.

4.2 The Rain/Snow Line

The traditional way of discriminating between rain and snow is examining the 1000-500 mb thickness value. A thickness value of 5400 m is considered to delineate the rain/snow line. However, this value is valid only for continental stations below 1000 ft elevation. For example, Ferber et al. (1993) stated that 5230 m is the mean rain/snow thickness value for Seattle, WA; they attributed the lower value to maritime influence. Other limitations of using the 1000-500 mb thickness value as a predictor include the 1000 mb surface being below ground as a winter storm approaches even if the station is near sea level, and the thickness value possibly not reflecting shallow warm layers near the surface.

Other thickness layers have been examined for their forecast potential as rain/snow discriminators. Keeter and Cline (1991) found that the 1000-700 mb thickness was best at distinguishing snow from rain across North Carolina. Heppner (1992) stressed the 850-700 mb thickness as the first parameter to examine in forecasting precipitation type. Koontz (1986) listed various thickness layers and their critical values for United States stations at low elevations, which are given in Table 12. If the thickness value is above the critical value, rain can be expected; if it is below the critical value, snow can be expected.

Table 12. Thickness layers and the corresponding critical thickness values to discriminate between rain and snow in the United States

| <i>Thickness layer (mb)</i> | <i>Thickness value (m)</i> |
|-----------------------------|----------------------------|
| 1000-850 | 1300 |
| 1000-700 | 2840 |
| 1000-500 | 5400 |
| 850-700 | 1540 |
| 850-500 | 4100 |
| 700-500 | 2560 |

Younkin developed a "snow index" based on the 850-700 mb and 1000-850 mb thicknesses (Brenton 1973). The index is

$$Y+2X=4179, \quad (17)$$

where

$$\begin{aligned} Y &= 850-700 \text{ mb thickness (m)} \\ X &= 1000-850 \text{ mb thickness (m)} \end{aligned}$$

If $Y+2X > 4179$, rain can be expected. If $Y+2X < 4179$ and the 850-700 mb thickness is less than 1557, snow can be expected; if the 850-700 mb thickness is greater than 1557, ice pellets or freezing rain can be expected.

Another traditional way to determine whether rain or snow will fall has been to examine the 850 mb temperature. If the temperature is at or below 0°C, snow would be expected. As Heppner (1992) pointed out, though, this criterion does not work well when the atmosphere is unstable, such as with post-cold front precipitation; he documented several rain events with the 850 mb temperature below 0°C. The height of the freezing level is a better predictor since it specifies the depth of the warm layer near the surface. McNulty (1988) summarized a study on the probability of snow based on the freezing level height:

- below surface 100% probability of snow
- 12 mb (315 ft) above surface 90% probability of snow
- 25 mb (660 ft) above surface 70% probability of snow
- 35 mb (920 ft) above surface 50% probability of snow

On average, the freezing level must be at least 1200 ft AGL for snow to melt into rain.

Surface temperature by itself is a poor predictor of precipitation type. As Matsuo et al. (1981) pointed out, precipitation type is dependent on the surface relative humidity as well as the surface temperature. They documented several cases where snow was reported when the surface temperature was greater than freezing but the relative humidity was low. Converting their surface temperatures and relative humidities to wet bulb temperatures, it can be seen that most of their snow cases occurred with a wet bulb temperature below 0°C. Expanding on their work, Heppner (1992) stated that the surface wet bulb temperature is a good predictor of precipitation type because it takes diabatic processes into account. He documented three

cases of rain when the 850 mb temperature and 850-700 mb thickness values indicated snow, but the surface wet bulb temperature was above freezing.

4.3 Freezing Rain and Ice Pellets

Freezing rain and ice pellets (also called sleet) occur when there is a warm layer (temperature greater than 0°C) above the surface, but the near-surface layer is below freezing. Ice pellets fall when snow does not completely melt in the warm layer and refreezes near the surface. Freezing rain falls when snow melts in the warm layer, becomes supercooled in the cold layer near the surface, and freezes on contact with the surface.

The rules of thumb for freezing rain are:

- surface temperature less than 0°C
- 1000-850 mb thickness in the range 1280-1310 m
- 850-700 mb thickness in the range 1540-1560 m
- 1000-700 mb thickness in the range 2825-2860 (Koontz 1986, Keeter and Cline 1991).

McNulty (1988) stated that freezing rain would occur with an elevated warm layer if the near-surface temperature was between 0°C and -10°C ; if the near-surface temperature was less than -10°C the melted snow would refreeze before reaching the surface. Stewart and King (1987) showed that the maximum temperature in the warm layer determined the precipitation type (snowflake size less than 3 mm):

- $T > 3.0^{\circ}\text{C}$ freezing rain
- $1.0^{\circ}\text{C} > T > 3.0^{\circ}\text{C}$ mixed precipitation (snow, rain, ice pellets)
- $T < 0.8^{\circ}\text{C}$ snow

Murphy (1988) reprinted previous studies showing that freezing rain can be expected when:

- surface wet bulb temperature $< -0.1^{\circ}\text{C}$ and 850 mb wet bulb temperature $> -1.5^{\circ}\text{C}$
- surface temperature is in the range -10°C - 0°C , and 850 mb temperature $> 0^{\circ}\text{C}$ (mixed precipitation can be expected with 850 mb temperature in range -7.5°C - 0°C).

The ideal ranges of various parameters for freezing rain and ice pellets are:

- surface temperature 0 to -4°C
- surface dew point 0 to -5°C
- 850 mb temperature $+1$ to $+6^{\circ}\text{C}$
- 1000-500 mb thickness 5330 to 5440 m
- dew point depression 850 mb: $< 1^{\circ}\text{C}$
surface: $< 3^{\circ}\text{C}$

Based on the discussion in Pruppacher and Klett (1978), Czys et al. (1996) have proposed a nondimensional parameter τ that would discriminate between freezing rain and ice pellets. It is the ratio of the time an ice particle is resident in the elevated warm layer and the time it takes for the maximum sized ice particle to completely melt:

$$\tau = \frac{\Delta Z_w k_w a}{(U(a) - \bar{V}) L_f \rho_i \int_a^0 \frac{r(a-r) dr}{T_0 - T_a(r)}}, \quad (18)$$

where

- ΔZ_w = thickness of warm layer
- k_w = thermal conductivity of water
- a = maximum ice particle radius
- $U(a)$ = terminal fall speed of ice particle
- \bar{V} = mean vertical air motion (assumed to be zero)
- L_f = latent heat of fusion
- ρ_i = density of ice
- r = ice core radius of partially melted ice particle
- T_0 = temperature at ice/water interface of ice particle
- $T_a(r)$ = temperature at particle/environment interface

$U(a)$ can be approximated by

$$U(a) = c_1 - c_2 \exp(-c_3 a), \quad (19)$$

where

- c_1 = 9.65 m sec⁻¹
- c_2 = 10.30 m sec⁻¹
- c_3 = 1200 m⁻¹

$T_a(r)$ can be found iteratively from

$$\frac{4\pi a k_w r [T_0 - T_a(r)]}{(a-r)} = 4\pi a k_a [T_\infty - T_a(r)] \bar{f}_h - 4\pi a L_v D_v (\rho_{v\infty} - \rho_{va}) \bar{f}_v, \quad (20)$$

where

- k_a = thermal conductivity of air
- T_∞ = temperature of environment
- \bar{f}_h = ventilation coefficient for heat
- L_v = latent heat of vaporization
- D_v = diffusivity of vapor
- $\rho_{v\infty}$ = vapor density of environment
- ρ_{va} = saturation vapor density at particle's surface
- \bar{f}_v = ventilation coefficient for vapor

For $\tau < 1$, ice pellets can be expected; for $\tau \geq 1$, freezing rain can be expected. When there is no warm layer, $\tau=0$ and snow can be expected.

4.4 Snow Accumulation

Snow accumulation is difficult to estimate exactly because the water vapor content of snow varies greatly. Light fluffy snow may only have a snow-to-water content ratio of 30:1 – that is, 30 inches of snow will melt to 1 inch of water. Wet snow may have a snow-to-water content ratio of up to 4:1. The traditional way to estimate snow amount is to calculate the precipitable water and assume a snow-to-water content ratio of 10:1.

The Cook Snow Index (Cook 1980) estimates the average amount of snow expected based on the 200 mb warm advection. Given that 700 mb warm advection is occurring, the average snowfall in inches for the next 24 hours will be about one-half of the maximum warm advection in degrees C expected at 200 mb. Naistat (1988) noted that the absolute difference of warm advection often yields the maximum amount of snowfall.

Visibility may be used as an estimate of snowfall rate (Brenton 1973). Table 13 lists the expected hourly snow accumulation based on the visibility.

Table 13. Surface visibility during snowfall and average hourly snow accumulation

| <i>Visibility</i> | <i>Average Hourly Accumulation</i> |
|-------------------|------------------------------------|
| > 5/8 mile | 0.2 inches |
| 5/16 mi to 5/8 mi | 1.0-1.2 in |
| <5/16 mi | 1.6 in |

Note that one must forecast the duration of the visibility restriction in order to estimate the total snow accumulation.

The National Weather Service has developed several empirical methods to forecast the location of the heavy snow band in a storm, where heavy snow is defined as 4 or more inches of snow in a 12-hour period or 6 or more inches of snow in a 24-hour period. Some of the methods of interest to the single-station forecaster include (Goetsch 1987):

- at 850 mb, the heavy snow band lies between the -2°C and the -8°C isotherms; the -5°C isotherm bisects the heavy snow band.
- at 700 mb, the heavy snow band lies between the -6°C and the -8°C isotherms and where the dewpoint temperature > -10°C.
- at 500 mb, the heavy snow band lies between -20°C and -25°C.
- 1000-500 mb relative humidity ≥ 80% for heavy snow
- 1000-500 mb thickness between 5310 and 5370 m for heavy snow
- 850-700 mb thickness between 1520 and 1540 m for heavy snow (Naistat 1988)
- the "Magic Chart": heavy snow lies in the area where the 850 mb temperature is between 0°C and -10°C, and the net vertical displacement in a 12-hour period of a parcel arriving at 700 mb is forecasted to be ≥ 80 mb (Sangster and Jagler 1985).

Lightning and thunder have been observed with snowstorms. Stewart and King (1990) concluded that winter thunder in the Toronto, Ontario region was associated with the mixed

precipitation region of a snowstorm. Winter snowstorms with thunder (popularly known as *thundersnow*) are also associated with *snow bursts*, when the snowfall rate exceeds one inch per hour. For example, Moore and Blakley (1988) reported that St. Louis, MO had over 25 cm (10 in) of snow accompanied by five hours of thunder and lightning in a 1982 snowstorm. Browning (1996) documented a 1995 snowstorm with thunder in Milwaukee, WI that dropped 7 in of snow in five hours. Single-station forecasters need to monitor stability indices even in winter to determine the possibility of convective activity with snowstorms.

5. SUMMARY

This report has presented a compilation of objective methods and “rules of thumb” that have been developed for forecasting thunderstorms, fog, and winter precipitation. It is the result of a search that concludes with the literature published through mid-1997. Section 6 provides an extensive bibliography for each of the meteorological events discussed.

6. BIBLIOGRAPHY

6.1 Introductory References

Oliver, V. J., and M. B. Oliver, 1945: Weather analysis from single-station data. In *Handbook of Meteorology*, eds. F. A. Berry, E. Bolay, and N. R. Beers, McGraw-Hill Book Co., 858-879.

6.2 Thunderstorm References

Air Weather Service, 1979: *The Use of the Skew T, log p Diagram in Analysis and Forecasting*. AWS/TR-79/006 (revised 1990), 153 pp.

Baker, D. V., and T. W. Schlatter, 1986: Private communication.

Banta, R. M., and C. B. Schaaf, 1987: Thunderstorm genesis zones in the Colorado Rocky Mountains as determined by traceback of geosynchronous satellite images. *Mon. Wea. Rev.*, **115**, 463-476.

Braham, R. R. Jr., 1996: The Thunderstorm Project. *Bull. Amer. Meteor. Soc.*, **77**, 1835-1845.

Brooks, H. E., C. A. Doswell III, and J. Cooper, 1994: On the environments of tornadic and nontornadic mesocyclones. *Wea. Forecasting*, **9**, 606-618.

Carlson, T. N., and F. H. Ludlam, 1968: Conditions for the occurrence of severe local storms. *Tellus*, **20**, 203-226.

Colquhoun, J. R., 1987: A decision tree method of forecasting thunderstorms, severe thunderstorms and tornadoes. *Wea. Forecasting*, **2**, 337-345.

Colquhoun, J. R., and P. R. Riley, 1996: Relationships between tornado intensity and various wind and thermodynamic variables. *Wea. Forecasting*, **11**, 360-371.

Davies-Jones, R., D. Burgess, and M. Foster, 1990: Test of helicity as a tornado forecast parameter. *Preprints, 16th Conf. Severe Local Storms*, Kananaskis Park, Alberta, Amer. Meteor. Soc., 588-592.

Dessens, J., and J. T. Snow, 1989: Tornadoes in France. *Wea. Forecasting*, **4**, 110-132.

Doswell, C. A. III, 1982: The operational meteorology of convective weather. Vol. I: Operational mesoanalysis. NOAA Tech. Memo. NWS NSSFC-5, 158 pp.

Doswell, C. A. III, 1991: A review for forecasters on the application of hodographs to forecasting severe thunderstorms. *Nat. Wea. Dig.*, **16**, (1), 2-16.

Doswell, C. A. III, and L. R. Lemon, 1979: An operational evaluation of certain kinematic and thermodynamic parameters associated with severe thunderstorm environments.

Preprints, 11th Conf. Severe Local Storms, Kansas City, MO, Amer. Meteor. Soc., 397-402.

Doswell, C. A. III, J. T. Schaefer, D. W. McCann, T. W. Schlatter, and H. B. Wobus, 1982: Thermodynamic analysis procedures at the National Severe Storms Forecast Center. *Preprints, Ninth Conf. Wea. Forecasting and Analysis*, Seattle, WA, Amer. Meteor. Soc., 304-309.

Doswell, C. A. III, F. Caracena, and M. Magnano, 1985: Temporal evolution of 700-500 mb lapse rate as a forecasting tool – A case study. *Preprints, 14th Conf. Severe Local Storms*, Indianapolis, IN, Amer. Meteor. Soc., 398-401.

Doswell, C. A. III, and E. N. Rasmussen, 1994: The effect on neglecting the virtual temperature correction on CAPE calculations. *Wea. Forecasting*, **9**, 625-629.

Graziano, T. M., and T. N. Carson, 1987: A statistical evaluation of lid strength on deep convection. *Wea. Forecasting*, **2**, 127-139.

Gulezian, D. P., 1980: Severe weather checklist used at National Weather Service Forecast Office, Portland, Maine. *Bull. Amer. Meteor. Soc.*, **61**, 1592-1599.

Hagemeyer, B. C., and G. K. Schmocker, 1993: Characteristics of east central Florida tornado environments. In *the Tornado: Its Structure, Dynamics, Prediction, and Hazards*, Geophys. Monogr. 79, Amer. Geophys. Union, 625-632.

Hales, J. E., 1985: Synoptic features associated with Los Angeles tornado occurrences. *Bull. Amer. Meteor. Soc.*, **66**, 657-662.

Hales, J. E., and C. A. Doswell III, 1982: High resolution diagnosis of instability using hourly surface lifted parcel temperatures. *Preprints, 12th Conference on Severe Local Storms*, Jan 11-15, San Antonio, TX, Amer. Meteor. Soc., 172-175.

Hart, J. A., and W. K. Korotky, 1991: The SHARP Workstation – v.1.50. A skew T/hodograph analysis and research program for the IBM and compatible PC. User's Manual. NOAA/NWS Forecast Office, Charleston, WV, 62 pp.

Henz, J. F., 1972: An operational technique of forecasting thunderstorms along the lee slopes of a mountain range. *J. Appl. Meteor.*, **11**, 1284-1292.

Hirt, W. D., 1985: Forecasting severe weather in North Dakota. *Preprints, 14th Conf. Severe Local Storms*, Indianapolis, IN, Amer. Meteor. Soc., 328-331.

Huntrieser, H., H. H. Schiesser, W. Schmid, and A. Waldvogel, 1997: Comparison of traditional and newly developed thunderstorm indices for Switzerland. *Wea. Forecasting*, **12**, 108-125.

- Jacovides, C. P., and T. Yonetani, 1990: An evaluation of stability indices for thunderstorm prediction in greater Cyprus. *Wea. Forecasting*, **5**, 559-569.
- Johns, R. H., 1986: Private communication.
- Johns, R. H., and C. A. Doswell III, 1992: Severe local storms forecasting. *Wea. Forecasting*, **7**, 588-612.
- Johns, R. H., J. M. Davies, and P. W. Leftwich, 1993: Some wind and instability parameters associated with strong and violent tornadoes. 2. Variations in the combinations of wind and instability parameters. In *the Tornado: Its Structure, Dynamics, Prediction, and Hazards*, Geophys. Monogr. 79, Amer. Geophys. Union, 583-590.
- Ludlam, F. H., 1963: Severe local storms: A review. *Meteor. Monogr.*, **5**, 27, Boston, MA, Amer. Meteor. Soc., 1-30.
- Maddox, R. A., and C. A. Doswell III, 1982: Forecasting severe thunderstorms: A brief consideration of some accepted techniques. *Nat. Wea. Dig.*, **7**, 2, 26-31.
- McGinley, J., 1986: Nowcasting mesoscale phenomena. In *Mesoscale Meteorology and Forecasting*, ed. P. S. Ray, Amer. Meteor. Soc., Boston, 657-688.
- McNulty, R. P., 1985: A conceptual approach to thunderstorm forecasting. *Nat. Wea. Dig.*, **10**, 2, 26-30.
- McNulty, R. P., 1995: Severe and convective weather: A Central Region forecasting challenge. *Wea. Forecasting*, **10**, 187-202.
- Miller, R. C., 1972: Notes on analysis and severe-storm procedures of the Air Force Global Weather Central. AWS Tech. Report 200 (Rev), 181 pp.
- Modahl, A. C., 1979: Synoptic parameters as discriminators between hailfall and less significant convective activity in northeast Colorado. *J. Appl. Meteor.*, **18**, 671-681.
- Moller, A. R., C. A. Doswell III, M. P. Foster, and G. R. Woodall, 1994: The operational recognition of supercell thunderstorm environments and storm structures. *Wea. Forecasting*, **9**, 327-347.
- Monteverdi, J. P., and J. Quadros, 1994: Convective and rotational parameters associated with three tornado episodes in northern and central California. *Wea. Forecasting*, **9**, 285-300.
- Monteverdi, J. P., and S. Johnson, 1996: A supercell thunderstorm with hook echo in the San Joaquin Valley, California. *Wea. Forecasting*, **11**, 246-261.
- Moore, J. T., and J. P. Pino, 1990: An interactive method for estimating maximum hailstone size from forecast soundings. *Wea. Forecasting*, **5**, 508-525.

- National Weather Service, 1984: Convective stability indices. NWS Western Region Tech. Attach. 84-14, 8 pp.
- Petterssen, S., 1956: *Weather Analysis and Forecasting, 2nd Edition. Volume II: Weather and Weather Systems*. McGraw-Hill Book Co., New York, 266 pp.
- Rife, D. L., 1996: The effects of mountains and complex terrain on airflow and development of clouds and precipitation. NWS Western Region Tech. Attach. 96-16, 5 pp.
- Sangster, W. E., and J. T. Schaefer, 1984: Nocturnal thunderstorms. NWS Central Region Tech. Attach. 84-10, 5 pp.
- Schaefer, J. T., 1986: The dryline. In *Mesoscale Meteorology and Forecasting*, ed. P. S. Ray, Amer. Meteor. Soc., 549-572.
- Swanson, B., 1990: Convective techniques (A springtime primer). 3rd Weather Wing Forecaster Memo 90/002, 16 pp.
- Tudurí, E., and C. Ramis, 1997: The environments of significant convective events in the western Mediterranean. *Wea. Forecasting*, **12**, 294-306.
- US Dept. of Commerce, 1969: *Radiosonde Observations*. Federal Meteorological Handbook No. 3, NAVAIR 50-1D-3.
- Walsh, J.E., 1974: Sea breeze theory and applications. *J. Atmos. Sci.*, **31**, 2012-2026.
- Weinbrecht, C. E., 1987: Mixing ratio – A clue to short term development. NWS Central Region Tech. Attach. 87-8, 13 pp.
- Weisman, M. L., and J. B. Klemp, 1982: The dependence of numerically simulated convective storms on vertical wind shear and buoyancy. *Mon. Wea. Rev.*, **110**, 504-520.
- Weisman, M. L., and J. B. Klemp, 1984: The structure and classification of numerically simulated convective storms in directionally varying wind shears. *Mon. Wea. Rev.*, **112**, 2479-2498.
- Weisman, M. L., and J. B. Klemp, 1986: Characteristics of isolated convective storms. In *Mesoscale Meteorology and Forecasting*, ed. P. S. Ray, Amer. Meteor. Soc., 331-358.

6.3 Fog References

- Air Weather Service, 1954: *General Aspects of Fog and Stratus Forecasting*. AWS TR 239, Scott AFB, IL, 99 pp.

- Air Weather Service, 1979: *The Use of the Skew T, Log p Diagram in Analysis and Forecasting*. AWS/TR-79/006 (revised 1990), Scott AFB, IL, 153 pp.
- Byers, H. R., 1959: *General Meteorology*. McGraw Hill Book Co., New York, 540 pp.
- Carpenter, A. B., 1941: A study of pre-warm frontal fog at Portland, Oregon. *Bull. Amer. Meteor. Soc.*, **22**, 47-51.
- Dightman, R. A., 1941: Fog and low stratus at Spokane, Washington. *Bull. Amer. Meteor. Soc.*, **22**, 309-314.
- Domrös, M., and P. Gongbing, 1988: *The Climate of China*. Springer-Verlag, Berlin, 361 pp.
- Donahue, C. A., K. M. Traxler, K. R. Walters, J. W. Louer III, M. T. Gilford, M. E. Edwards, J. L. Harding, R. C. Bonam, and S. A. Straw, 1995: *Equatorial Africa: A Climatological Study*. USAF Environmental Technical Applications Center, Scott AFB, IL, USAFETAC/TN-95/001, 258 pp.
- Federal Aviation Agency and Department of Commerce, 1965: *Aviation Weather for Pilots and Flight Operations Personnel*. Superintendent of Documents, US Government Printing Office, Washington, DC, 299 pp.
- Felsch, P., and W. Whitlatch, 1993: Stratus surge prediction along the central California coast. *Wea. Forecasting*, **8**, 204-213.
- Fitzjarrald, D. R., and G. G. Lala, 1989: Hudson Valley fog environments. *J. Appl. Meteor.*, **28**, 1303-1328.
- George, J. J., 1951: Fog. In *Compendium of Meteorology*, ed. T. F. Malone, Amer. Meteor. Soc., Boston, 1179-1189.
- Gilford, M. T., M. J. Vojtesak, G. Myles, R. C. Bonam, and D. L. Martens, 1992: *South America South of the Amazon River, A Climatological Study*. USAF Environmental Technical Applications Center, Scott AFB, IL, USAFETAC/TN-92/004, 689 pp.
- Guttman, N. B., 1971: *Study of Worldwide Occurrence of Fog, Thunderstorms, Supercooled Low Clouds and Freezing Temperatures*. U.S. Naval Weather Service Command, NAVAIR 50-1C-60, 67 pp.
- Holets, S., and R. N. Swanson, 1981: High-inversion fog episodes in central California. *J. Appl. Meteor.*, **20**, 890-899.
- Huschke, R. E., Ed., 1959: *Glossary of Meteorology*. Amer. Meteor. Soc., Boston, 638 pp.
- Jannuzzi, J. A., 1993: The onshore push of marine air into the Pacific Northwest. *Wea. Forecasting*, **8**, 194-203.

- Jannuzzi, J. A., 1997: Personal communication.
- Kendrew, W. G., 1961: *The Climates of the Continents*, 5th ed. Oxford University Press, London, 608 pp.
- Kinzebach, R. M., 1955: An objective method of forecasting the occurrence of low clouds in the McChord-Seattle area during the summer months. *Bull. Amer. Meteor. Soc.*, **36**, 104-108.
- Leipper, D. F., 1994: Fog on the U. S. West Coast: A review. *Bull. Amer. Meteor. Soc.*, **75**, 229-240.
- Leipper, D. F., 1995: Fog forecasting objectively in the California coastal area using LIBS. *Wea. Forecasting*, **10**, 741-762.
- List, R. J., 1963: *Smithsonian Meteorological Tables*, 6th Ed. Smithsonian Institution, Washington, DC, 527 pp.
- Mass, C. F., M. D. Albright, and D. J. Brees, 1986: The onshore surge of marine air into the Pacific Northwest: A coastal region of complex terrain. *Mon. Wea. Rev.*, **114**, 2602-2627.
- Mass, C. F., and M. D. Albright, 1987: Coastal southerlies and alongshore surges of the West Coast of North America: Evidence of mesoscale topographically trapped response to synoptic forcing. *Mon. Wea. Rev.*, **115**, 1707-1738.
- McGinley, J., 1986: Nowcasting mesoscale phenomena. In *Mesoscale Meteorology and Forecasting*, ed. P. S. Ray, Amer. Meteor. Soc., Boston, 657-688.
- Meyer, M. B., and G. G. Lala, 1990: Climatological aspects of radiation fog occurrence at Albany, New York. *J. Climate*, **3**, 577-586.
- Naistat, R. J., 1988: Forecasting fog dissipation the old-fashioned way. NWS Central Region Tech. Attach. 88-25, 13 pp.
- Noonkester, V. R., 1979: Coastal marine fog in southern California. *Mon. Wea. Rev.*, **107**, 830-851.
- Petterssen, S., 1956: *Weather Analysis and Forecasting*, 2nd Edition. Volume II: *Weather and Weather Systems*. McGraw-Hill Book Co., New York, 266 pp.
- Pilié, R. J., E. J. Mack, W. C. Kocmond, C. W. Rogers, and W. J. Eadie, 1975: The life cycle of valley fog. Part I: Micrometeorological characteristics. *J. Appl. Meteor.*, **14**, 347-363.

- Pilié, R. J., E. J. Mack, C. W. Rogers, U. Katz, and W. C. Kocmond, 1979: The formation of marine fog and the development of fog-stratus systems along the California coast. *J. Appl. Meteor.*, **18**, 1275-1286.
- Ramage, C. S., 1954: Non-frontal crachin and the cool season clouds of the China Seas. *Mon. Wea. Rev.*, **35**, 404-411.
- Ramage, C. S., 1971: *Monsoon Meteorology*. Academic Press, New York, 296 pp.
- Reason, C. J. C., and M. R. Jury, 1990: On the generation and propagation of the southern African coastal low. *Q. J. Roy. Meteor. Soc.*, **116**, 1133-1151.
- Taljaard, J. J., 1972: Synoptic meteorology of the Southern Hemisphere. In *Meteorology of the Southern Hemisphere*, ed. C. W. Newton. *Meteor. Monogr*, **13**, no. 35, Amer. Meteor. Soc., Boston, 139-213.
- Traxler, K. M., R. D. Arnold, J. W. Louer III, M. T. Gilford, K. R. Gibson, R. C. Bonam, and K. R. Walters, 1993: *Eastern Europe: A Climatological Study*. USAF Environmental Technical Application Center, Scott AFB, IL, USAFETAC/TN-93/004, 373 pp.
- Traxler, K. M., R. D. Arnold, J. W. Louer, M. T. Gilford, J. L. Harding, R. C. Bonam, K. R. Walters, C. A. Donahue, 1994: *Southern Africa: A Climatological Study*. USAF Environmental Technical Application Center, Scott AFB, IL, USAFETAC/TN-94/005, 200 pp.
- Vojtesak, M. J., K. P. Martin, G. Myles, M. T. Gilford, and K. R. Gibson, 1991: *SWANEA: A Climatological Study. Volume II — The Middle East Peninsula*. USAF Environmental Technical Application Center, Scott AFB, IL, USAFETAC/TN-91/002 (revised), 248 pp.
- Woodward, W. H., 1941: Fog and stratus at Seattle. *Bull. Amer. Meteor. Soc.*, **22**, 242-249.
- Zhang, J., and Z. Lin, 1992: *Climate of China* (trans. D. Tan). John Wiley and Sons, New York, 376 pp.

6.4 Winter Precipitation References

- Bocchieri, J. R., 1980: The objective use of upper air soundings to specify precipitation type. *Mon. Wea. Rev.*, **108**, 596-603.
- Brenton, C. L., 1973: A resume on the state of the art for snow forecasting. USAF Environmental Technical Applications Center, Scott AFB, IL, USAFETAC TN 73-6, 27 pp.
- Browning, W. D., 1996: The Milwaukee snowstorm of November 27, 1995. NWS Central Region Tech. Attach. 96-08, 4 pp.

- Cook, B. J., 1980: A snow index using 200 mb warm advection. *Nat. Wea. Dig.*, **5**, 29-40.
- Czys, R. R., R. W. Scott, K. C. Tang, R. W. Przybylinski, and M. E. Sabones, 1996: A physically based, nondimensional parameter for discriminating between locations of freezing rain and ice pellets. *Wea. Forecasting*, **11**, 591-598.
- Drake, J. C., and B. J. Mason, 1966: The melting of small ice spheres and cones. *Q. J. Roy. Meteor. Soc.*, **92**, 500-509.
- Ferber, G. K., C. F. Mass, G. M. Lackmann, and M. W. Patnoe, 1993: Snowstorms over the Puget Sound lowlands. *Wea. Forecasting*, **8**, 481-504.
- Figurskey, D., 1994: The use of 925 mb temperature data in diagnosing winter precipitation type. NWS Central Region Tech. Attach. 94-17, 10 pp.
- Goetsch, E. H., 1987: Checklist of significant winter weather forecasting techniques – A summary of some long-established methods. NWS Central Region Tech. Attach. 87-30, 5 pp.
- Heppner, P. O. G., 1992: Snow versus rain: Looking beyond the "magic" numbers. *Wea. Forecasting*, **7**, 683-691.
- Keeter, K. K., and J. W. Cline, 1991: The objective use of observed and forecast thickness values to predict precipitation type in North Carolina. *Wea. Forecasting*, **6**, 456-469.
- Keeter, K. K., S. Businger, L. G. Lee, and J. S. Waldstreicher, 1995: Winter weather forecasting throughout the eastern United States. Part III: The effects of topography and the variability of winter weather in the Carolinas and Virginia. *Wea. Forecasting*, **10**, 42-60.
- Koontz, G., 1986: Heavy snow forecasting aids. NWS Central Region Tech. Attach. 86-26, 3 pp.
- Maglaras, G. J., J. S. Waldstreicher, P. J. Kocin, A. F. Gigi, and R. A. Marine, 1995: Winter weather forecasting throughout the eastern United States. Part I: An overview. *Wea. Forecasting*, **10**, 5-20.
- Matsuo, T., Y. Sasyo, and Y. Sato, 1981: Relationship between types of precipitation on the ground and surface meteorological elements. *J. Meteor. Soc. Japan*, **59**, 462-476.
- McNulty, R. P., 1988: Winter precipitation type. NWS Central Region Tech. Attach. 88-4, 9 pp.
- Moore, J. T., and P. D. Blakley, 1988: The role of frontogenetical forcing and conditional symmetric instability in the Midwest snowstorm of 30-31 January 1982. *Mon. Wea. Rev.*, **116**, 2155-2171.

- Murphy, J. D., 1988: Winter precipitation. USAF 5th Wea. Wing, Langley AFB, VA, 5WW/FM-88/004, 112 pp.
- Naistat, R. J., 1988: Using mid-level thickness patterns and warm air advection to forecast heavy snow. NWS Central Region Tech. Attach. 88-36, 10 pp.
- Pruppacher, H. R., and J. D. Klett, 1978: *Microphysics of Clouds and Precipitation*. D. Reidel Publishing Co., Dordrecht, Holland, 714 pp.
- Sangster, W. E., and E. C. Jagler, 1985: The (7WG, 8WT) Magic Chart. NWS Central Region Tech. Attach. 85-1, 5 pp.
- Steigerwaldt, H., and R. Przybylinski, 1983: A brief discussion of various "rules of thumb" and their application to the winter storm of December 16-17, 1981. NWS Central Region Tech. Attach. 83-13, 7 pp.
- Stewart, R. E., and P. King, 1987: Freezing precipitation in winter storms. *Mon. Wea. Rev.*, **115**, 1270-1279.
- Stewart, R. E., and P. King, 1990: Precipitation type transition regions in winter storms over southern Ontario. *J. Geophys. Res.*, **95**, 22355-22368.